THIS IS THE ACCEPTED VERSION OF THE FOLLOWING ARTICLE:
A. C. Anselmo, X. Xu, S. Buerkli, Y. Zeng, W. Tang, K. J. McHugh, A. M. Behrens, E. Rosenberg, A. R. Duan, J. L. Sugarman, J. Zhuang, J. Collins, X. Lu, T. Graf, S. Y. Tzeng, S. Rose, S. Acolatse, T. D. Nguyen, X. Le, A. S. Guerra, L. E. Freed, S. B. Weinstock, C. B. Sears, B. Nikolic, L. Wood, P. A. Welkhoff, J. D. Oxley, D. Moretti, M. B. Zimmermann, R. Langer, A. Jaklenec,
A heat-stable microparticle platform for oral micronutrient delivery. Sci. Transl. Med. 11, eaaw3680 (2019)., which has been published in final form at
https://stm.sciencemag.org/content/11/518/eaaw3680

Title: A heat-stable microparticle platform for oral micronutrient delivery

Authors: Aaron C. Anselmo[1,§,†], Xian Xu[1,§], Simone Buerkli[2,§], Yingying Zeng[1], Wen Tang[1], Kevin J. McHugh[1,#], Adam M. Behrens[1], Evan Rosenberg[1], Aranda R. Duan[1], James L. Sugarman[1], Jia Zhuang[1], Joe Collins[1], Xueguang Lu[1], Tyler Graf[1], Stephany Y. Tzeng[1], Sviatlana Rose[1], Sarah Acolatse[1], Thanh D. Nguyen[1,‡], Xiao Le[1], Ana Sofia Guerra[3], Lisa E. Freed[1,¥], Shelley B. Weinstock[4], Christopher B.Sears[5], Boris Nikolic[6], Lowell Wood[7], Philip A. Welkhoff[7], James D. Oxley[8], Diego Moretti[2,‡], Michael B. Zimmermann[2], Robert Langer[1*], and Ana Jaklenec[1*]

[§]These authors contributed equally to this manuscript.

Affiliations:

1. David H. Koch Institute for Integrative Cancer Research, Massachusetts Institute of Technology, Cambridge, MA 02139, USA
2. Institute of Food Nutrition and Health, ETH Zurich, 8092, Switzerland
3. Department of Chemistry & Chemical Biology, Harvard University, Cambridge, MA 02138, USA
4. Institute of Human Nutrition, Columbia University College of Physicians and Surgeons, NY, 10032 USA
5. Independent Scholar, Belmont, MA 02478, USA
6. Biomatics Capital, 1107 1st Avenue, Apartment 1305, Seattle, WA 98101, USA.
7. Institute for Disease Modeling, Bellevue, WA 98005, USA.
8. Southwest Research Institute, San Antonio, TX 78238 USA

† Present address: Division of Pharmacoengineering and Molecular Pharmaceutics, Eshelman School of Pharmacy, University of North Carolina at Chapel Hill, Chapel Hill, NC, 27599, USA.

Present address: Department of Bioengineering, Rice University, Houston, TX, 77030

‡ Present address: Department of Mechanical Engineering, University of Connecticut, Storrs, CT 06269, USA.

¥ Present address: Media Lab, Massachusetts Institute of Technology, Cambridge, Massachusetts, 02139, USA

[*] Corresponding author. Email: jaklenec@mit.edu (A.J.); rlanger@mit.edu (R.L.);

ǂ Present address: Nutrition Group, Health Department, Swiss Distance University of Applied Sciences, Regensdorf, CH-8105, Switzerland

One Sentence Summary: A heat-stable microparticle platform improves oral micronutrient delivery.

Abstract: Micronutrient deficiencies affect up to 2 billion people and are the leading cause of cognitive and physical disorders in the developing world. Food fortification is effective in treating micronutrient deficiencies; however, its global implementation has been limited by technical challenges in maintaining micronutrient stability during cooking and storage. We hypothesized that polymer-based encapsulation could address this and facilitate micronutrient absorption. We identified poly(butylmethacrylate-co-(2-dimethylaminoethyl)methacrylate-co-methylmethacrylate) (1:2:1), BMC, as a material with proven safety, offering stability in boiling water, rapid dissolution in gastric acid, and the ability to encapsulate distinct micronutrients. We encapsulated 11 micronutrients (iron, iodine, zinc, and vitamins A, B2, niacin, biotin, folic acid, B12, C, D), and co-encapsulated up to 4 micronutrients. Encapsulation improved micronutrient stability against heat, light, moisture, and oxidation. Rodent studies confirmed rapid micronutrient release in the stomach and intestinal absorption. Bioavailability of iron from microparticles, compared to free iron, was lower in an initial human study. An organotypic human intestinal model revealed increased iron loading and decreased polymer content would improve absorption. Using process development approaches capable of kg-scale synthesis, we increased iron loading over 30-fold. Scaled batches tested in a follow-up human study exhibited up to 89% relative iron

bioavailability compared to free iron. Collectively, these studies describe a broad approach for clinical translation of a heat-stable ingestible micronutrient delivery platform with the potential to improve micronutrient deficiency in the developing world. These approaches could potentially be applied towards clinical translation of other materials, such as natural polymers, for encapsulation and oral delivery of micronutrients.

Introduction

Micronutrient deficiencies are prevalent across the developing world, affecting 2 billion people (*1*) and causing cognitive and physical disorders such as anemia, blindness, birth defects, impaired growth in children (*2-7*), and around two million childhood deaths per year (*8-10*). Large-scale human trials have established that micronutrient fortification of foods can effectively treat micronutrient deficiencies (*11-18*), but this approach has been limited (*19-21*) due to poor implementation in certain countries and unaddressed technical challenges related to micronutrient stability during storage and cooking. For example, heat, moisture, and oxidation encountered during cooking can impair absorption of vitamins through degradation (*17, 18, 22-26*), or make food unpalatable through chemical changes to minerals (*27*). As such, the development of technologies that address these stability challenges can facilitate implementation of staple food fortification and impact global health by treating worldwide micronutrient deficiencies.

Current micronutrient technologies focus on encapsulation in microparticles (MPs), nanoparticles, agglomerates, and powders using biopolymers and food-additives such as proteins, polysaccharides, lipids, and surfactants (*28-33*). However, these approaches are limited in addressing the stability challenges encountered during end use of the micronutrients (cooking) and

delivery challenges related to micronutrient release and subsequent absorption by the body. We hypothesized that we could address this by using a pH-sensitive polymer that: encapsulates both water-soluble and fat-soluble micronutrients; protects the encapsulated micronutrient from high temperature, moisture, and oxidizing agents; and rapidly releases in the stomach to ensure intestinal absorption.

Using an encapsulating matrix, we describe a MP delivery platform that: encapsulates 11 micronutrients individually and up to 4 micronutrients in combination; enhances micronutrient stability after exposure to boiling water, light, or oxidizing chemicals found in common foods; and rapidly releases micronutrients upon exposure to simulated gastric fluid (SGF). In vivo studies confirmed rapid micronutrient release in the stomach and subsequent absorption in the small intestine. In humans, we investigated the bioavailability of ferrous sulfate (iron) after ingestion of iron-loaded MPs. Alongside complementary studies in an organotypic intestinal model, we identified MP iron loading and MP polymer content to be absorption limiting parameters in humans. We then developed and subsequently leveraged large-scale process development approaches to simultaneously increase loading and decrease polymer content in MPs. In a second human trial, MPs synthesized at scale with higher iron loading and lower polymer content demonstrated non-inferior absorption as compared to non-MP controls. These results indicate that this MP platform can be used to individually encapsulate or co-encapsulate micronutrients in a modular manner, maintain stability over 2 hours in boiling water, and then rapidly release in gastric conditions to successfully deliver micronutrients to humans. Overall, our study details a broad approach from conception to human trials of a highly heat-stable MP platform for oral micronutrient delivery.

Results

Formulation of MPs at laboratory scale

We initially considered over fifty potential polymers that could simultaneously be stable in boiling water and dissolve rapidly in low pH and closely evaluated ten candidates **(table S1)**. BMC [poly(butylmethacrylate-co-(2-dimethylaminoethyl)methacrylate-co-methylmethacrylate) (1:2:1)], available commercially as either a U.S. Food and Drug Administration (FDA)-approved inactive ingredient (Eudragit E PO-powder) or a self-affirmed generally recognized as safe (GRAS)-status material (Eudraguard Protect-powder) was selected as the MP encapsulation material as it simultaneously addresses the above challenges **(table S1)** (*34-41*). Micronutrients were encapsulated individually in MPs using a one-step **(Fig. 1A)** or two-step **(Fig. 1B)** emulsion process, followed by centrifugation to remove unencapsulated micronutrients. In both approaches, BMC was used as the encapsulant; however, the two-step process used either hyaluronic acid (HA) or gelatin (Ge) as an additional stabilizing excipient included in the first step **(Fig. 1B)**. For the two-step process, MPs sampled during the first step were about 5 μm in diameter **(Fig. 1C)** whereas after the second step they exhibited a hierarchical particle-in-particle structure about 200 μm in diameter **(Fig. 1, D and E)**. The two-step process was used for water-soluble micronutrients that could not be encapsulated using the one-step process, due to non-homogenous suspension of water-soluble micronutrients. This two-step approach was additionally used to enable the co-encapsulation of vitamins A, D, folic acid, and B12 **(fig. S1)**. In contrast, MPs synthesized via the one-step process exhibited homogeneous internal structure and were about 200 μm in diameter **(Fig. 1F)**. Formulation parameters, loadings, and encapsulation efficiencies for each of the lab-scale MPs are shown in **table S2**.

Controlled release of micronutrients in vitro

In vitro release studies confirmed the retention of micronutrients in the encapsulated MPs after exposure to room temperature (RT) water or boiling (100°C) water **(Fig. 2)**. pH-responsive burst release was exhibited when particles were exposed to 37°C SGF at pH 1.5 **(Fig. 2)**. Micronutrient retention during 2 h in boiling water was used as a baseline index of MP stability under simulated cooking conditions, since micronutrients such as vitamin A undergo chemical degradation when exposed to high temperature or humidity (*16, 17*). The one-step process was confirmed to achieve retention (>80% at 120 min) in 100°C or RT water and rapid release (>80% at 30 min) in 37°C SGF for most individually encapsulated micronutrients **(Fig. 2)**. The two-step process was developed to further stabilize highly water-soluble micronutrients within the BMC matrix **(Fig. 2)**. More specifically, when the two-step process that included HA as the stabilizing biopolymer was used to encapsulate $FeSO_4$, the payload was largely retained (>90% at 120 min) in 100°C or RT water and rapidly released (>80% at 30 min) in 37°C SGF, whereas $FeSO_4$ formulations synthesized via the one-step process exhibited payload release, even in RT water. The role of pH in modulating release kinetics was investigated using vitamin B12 as a representative micronutrient, where payload release was achieved more rapidly at lower pH values **(fig. S2)**. Time-lapse imaging of vitamin A-BMC MPs immersed in SGF exhibited payload release in <1 min **(Fig. 2B)**, as did Fe-HA-BMC MPs **(Fig. 2C)**. Four co-encapsulated vitamins, water-soluble vitamins B12 and folic acid introduced in step 1 and fat-soluble vitamins A and D introduced in step 2 **(fig. S1)**, each maintained payload retention (>80% at 120 min) in 100°C or RT water and rapidly released (60-90% at 30 min) the payloads in 37°C SGF **(Fig. 2, D-G)**. Together, these results indicate that the BMC MP platform system can be used to individually encapsulate or co-

encapsulate micronutrients in a modular manner, provide retention during 2 hours in boiling water, and enable burst release in 37°C SGF.

Micronutrient stability under heat, water, ultraviolet light, and oxidizing agents

Many micronutrients, such as vitamin A (*23*-*25*) and iron (*26*), are sensitive to high temperatures, moisture, ultraviolet light, or oxidizing chemicals, which can lead to degradation or changes in the oxidative states and thus limit absorption after ingestion (*26*). As such, we studied the role that BMC encapsulation plays in improving micronutrient stability against these challenges for both individually and co-encapsulated formulations. We first investigated protection of the micronutrient payload during 2 hours in boiling water, which exposed the payload to high temperatures and moisture. For the encapsulated fat-soluble micronutrients vitamin A and D, over 5- and 18-fold enhanced recovery was observed, respectively, as compared to unencapsulated counterparts **(Fig. 3A)**, after exposure to boiling water conditions for 2 hours. Similarly, encapsulation protected water-soluble vitamins C and B2 during boiling, as both water-soluble vitamin groups exhibited enhanced recovery as compared to unencapsulated controls **(Fig. 3A)**. We next investigated protection of the micronutrient payload after 24 hours of light exposure (280 $\mu W/cm^2$), since both vitamin A (*32*) and vitamin D (*42*) are rapidly degraded by ultraviolet light in their unencapsulated forms **(Fig. 3B)**. Recovery after light exposure was significantly improved by over 15- and 3-fold for vitamin A and D, respectively, encapsulated in BMC MPs as compared to unencapsulated controls **(Fig. 3B,** $P < 0.05$**)**.

Similar to individually-encapsulated micronutrients, co-encapsulated micronutrients maintained their biological activity after exposure to boiling water for up to 2 hours **(Fig. 3C)**. Negative oxidizing interactions between micronutrients in fortified products and micronutrients

naturally present in food sources readily occur, and these interactions can negatively impact absorption and bioavailability (*18*). For example, polyphenols present in food catalyze iron oxidation, resulting in a dramatic color change, from a highly bioavailable ferrous (Fe^{2+}) state to a ferric state (Fe^{3+}) (*43*) that exhibits poor bioavailability (*26*). To examine whether BMC encapsulation prevents interactions between the encapsulated iron and oxidizing chemicals present in food, BMC-encapsulated and unencapsulated iron was added to polyphenol-rich banana milk and the color change was quantified over time. Iron encapsulation in HA-BMC MPs exhibited less color change, and therefore less oxidation, in banana milk as compared to unencapsulated iron **(Fig. 3D)**. These results indicate that the BMC MP matrix can limit interactions between the encapsulated iron and the free polyphenols in food. Finally, to demonstrate a maintained capability for pH-controlled release of iron following exposure to high temperature, moisture, and oxygen, iron-loaded MPs that were first boiled for 2 hours and then immersed in SGF were visualized using real-time microscopy, confirming that they maintained their ability to rapidly release their iron payload at low pH **(Fig. 3E)**. After boiling, HA-BMC MPs retained similar morphology **(fig. S3)** to pre-boiling **(Fig. 1D)**. Overall, these results indicate that encapsulation in BMC protects micronutrient payloads during exposure to high temperatures, moisture, ultraviolet light, and oxidizing chemicals.

Release of a model payload and absorption of vitamin A in vivo

To confirm BMC MP dissolution in vivo, female SKH1-Elite mice were used to track payload release using the near infrared fluorescent dye 1,1'-Dioctadecyl-3,3,3',3'-Tetramethylindotricarbocyanine Iodide (DiR) encapsulated in BMC. DiR can be differentiated in the encapsulated and released states by investigating the influence of environmental conditions on

DiR's fluorescent properties using established imaging techniques (*44*). A 14-point spectral fingerprint of a DiR-loaded BMC MP was obtained when the MP was suspended in water. In contrast, when DiR is released from a BMC MP in SGF, the resulting blue shift exhibits a spectral profile distinct from encapsulated DiR. As such, the encapsulated and released DiR could be differentiated using their distinct fluorescent fingerprints **(fig. S4)**. The two fingerprints of the dye in either encapsulated or released form were used to indirectly reflect the dissolution of the BMC MPs in vivo. DiR-loaded BMC MPs were administered orally to mice, and at timed intervals the animals were euthanized and the complete gastrointestinal tract was excised for ex vivo fluorescence imaging **(Fig. 4A)**. Both the physical state of the dye (encapsulated or released) and the physiological location of the dye in the gastrointestinal tract were visualized **(Fig. 4A)** and quantified **(Fig. 4B)**. At 15 minutes, the stomach contained a mixture of encapsulated and released DiR, suggesting that the BMC MPs were partially dissolved and a portion of payload was released but had not yet entered the intestines. At 30 minutes, DiR signal was predominately detected as both encapsulated dye in the stomach and released dye in the intestines. At 60 minutes, minimal signal of BMC encapsulated DiR was detectable, highlighting how the majority of particles released their payload within 1 hour. Furthermore, at 1 hour the released dye signal was exclusively in the intestines, implying that the released payload had passed through the stomach and into the intestines within 1 hour. These findings confirm rapid release of a model payload from orally administered MP into the murine gastrointestinal tract. To determine whether this rapid release would facilitate absorption of encapsulated micronutrients, we evaluated the absorption of vitamin A in female Wistar rats. Tritium-labeled vitamin A was orally administrated to rats by gavage in both the free form and BMC-encapsulated forms and blood samples were taken to evaluate vitamin A content over a period of 6 hours **(Fig. 4C)**. Encapsulated vitamin A exhibited statistically

indistinguishable absorption relative to free vitamin A **(Fig. 4C)**, highlighting that encapsulation in BMC did not influence absorption.

Bioavailability of iron in humans and iron transport in an in vitro intestinal barrier model

Fe-HA-BMC MPs were investigated for their ability to deliver bioavailable iron in humans. Iron bioavailability was investigated through the consumption of 3 stable iron-isotope labeled test meals administered in a randomized single-blind, cross-over design to fasting young women [n=20 mean±SD hemoglobin (Hb) = 13.4 ± 0.85 g/L, and geometric mean (95%CI) plasma ferritin (PF) 11.6 (9.4, 14.5) μg/L] **(table S3)**. The test meals were whole-grain maize porridge with vegetable sauce, an iron-absorption inhibitory meal (*45*) with an iron:phytic acid molar ratio of 1:6.5 and negligible (0.4 mg/meal) ascorbic acid content, to which labeled unencapsulated or encapsulated ferrous sulfate was added after cooking. Two test meals contained 4 mg iron as labeled ferrous sulfate (either ^{54}Fe or ^{57}Fe) in HA-BMC MPs (encapsulated iron), which was added either before or after cooking, to investigate the effects that cooking (30 min baking at 100°C) had on iron bioavailability after MP encapsulation. The third test meal, the reference, contained 4 mg unencapsulated iron (free) as labeled ferrous sulfate (^{58}Fe). The geometric mean (95%CI) of fractional iron absorption (FIA) of the reference meal (free uncooked Fe) was 3.36 (2.29, 4.95)%, whereas the fractional iron absorption of ferrous sulfate from uncooked Fe-HA-BMC MPs was 1.46 (0.77, 2.79)% **(Fig. 5A)**. Fe-HA-BMC MPs exhibited 44 (22, 88)% relative iron bioavailability (RBV) as compared to unencapsulated ferrous sulfate ($P < 0.01$) **(Fig. 5A)**. Cooking the encapsulated ferrous sulfate had no effect on its bioavailability [FIA: 1.41 (0.91, 2.19)%, and RBV: 42 (34, 53)%] **(Fig. 5A)**.

Although the first human study showed that Fe encapsulation in HA-BMC MPs reduces iron bioavailability as compared to unencapsulated iron **(Fig. 5A)**, our platform demonstrated efficacy in delivering bioavailable iron to humans, independent of cooking conditions **(Fig. 5A)**. It has been previously reported that materials that encapsulate micronutrients can interfere with absorption (*15*); as such, we investigated the role that HA and BMC independently play in the intestinal absorption of iron. In vitro studies were designed to simulate conditions of iron penetration of the intestinal epithelial cell barrier in humans after oral ingestion of Fe-HA-BMC MPs. A commercially available human intestinal epithelial cell barrier model (EpiIntestinal, MatTek) provided a test platform to investigate the effect the MP constituents have on intestinal iron absorption by systematically varying the relative concentrations of iron, HA, and BMC. The model consisted of primary small intestine epithelial cells obtained from a healthy human donor, dissociated enzymatically, and cultured in customized medium on cell culture inserts within 12-well-plates to form a functional, columnar-like three dimensional (3D) epithelial barrier layer (*46*).

Oral administration of iron formulations was modeled by adding samples into the apical surface of the intestinal barrier, accessible as the cell culture insert in the upper compartment of the well-plate and, after a one hour incubation period, quantifying iron transport as the amount that passed through the tissue barrier and could be determined by analysis of the culture medium in the lower compartment of the well-plate. The transport of iron added in combination with HA **(Fig. 5B)** and/or BMC **(Fig. 5C)** was expressed as a percentage of the transport of free iron added in the absence of HA or BMC. HA presence exhibited no significant effect on iron transport through the intestinal barrier **(Fig. 5B)**. Moreover, iron was readily transported through the barrier at the Fe:HA ratio used in the MPs tested in this first human study. In contrast, unencapsulated BMC added to iron at increasing percentages significantly reduced iron transport through the intestinal barrier

(Fig. 5C). In particular, iron was poorly transported through the barrier when present at the BMC percentage of 96%, which corresponds to the percent BMC in the MPs tested in human subjects. At the percentage of BMC present in the current MP formulation, iron transport was reduced to 37% compared to free iron. Similarly, iron transport was reduced to 33% of that measured for free iron when the neutralized contents of MPs dissociated by incubation in SGF were added to the intestinal barrier **(Fig. 5C)**. Interestingly, as BMC percentage decreased the iron transport-inhibiting effects of BMC became negligible, which indicates that formulations containing lower percentage of BMC may not inhibit iron transport across the intestines. By using this organotypic model to determine the conditions that do not inhibit iron transport, we have highlighted the utility of in vitro models for use in screening micronutrient formulations to inform MP design (*47*).

Process development and scale-up

The MPs described were conceived and synthesized as lab-scale research formulations. Although emulsion-based microencapsulation methods are a staple in many biomaterial and formulation labs at the academic level (*28*, *48*), we encountered considerable challenges in increasing the iron loading when encapsulated in BMC. To address this, and to overcome the absorption issues that were encountered in the first human study, we developed new processes to increase the loading of iron in our formulation **(Fig. 6A)**. A commercially-available spray dryer and a customized spinning disc atomizer were used to formulate Fe-HA MPs **(Fig. 6B)** and Fe-HA-BMC MPs **(Fig. 6C)**, respectively, at the kilogram scale. The initial scaled formulation was designed to recreate the 0.6% iron loading used in the first human study. Batches of Fe-HA-BMC MPs produced at the pilot scale (> 1 kg) and at the same compositions of those used in the first human study met the same loading, stability, and pH controlled release criteria as the lab-scale formulation tested in

humans **(Fig. 6D)**. We further developed processes to increase the loading of iron in BMC particles to 3.19% **(fig. S5A)** and 18.29% **(fig. S5B)**, which additionally decreased BMC amounts **(table S4)**. These scaled and high-loaded iron BMC MPs exhibited near complete release of iron in SGF in less than 5 minutes **(fig. S5C)**. As expected, the release of iron in pH 5 buffered water demonstrated a pH-dependency **(fig. S5, A and B)**. For human studies, food grade iron-loaded BMC particles with acceptable values for residual dichloromethane (DCM), endotoxins, and microbial bioburden **(table S5)** were used. These scaled MPs were also examined for their ability to prevent interactions between the encapsulated iron and oxidizing chemicals present in food as described above with polyphenol-rich banana milk. It was demonstrated that the scaled Fe-HA-BMC MPs induced less color change as compared to all free forms of iron, both with and without the other MP constituents (HA, BMC, HA with BMC) **(fig. S5D)**.

Bioavailability of iron particles of 5- and 30-fold higher loading in humans

Fe HA-BMC MPs at over 5-fold and over 30-fold higher iron loading, compared to the lab-scale batch used in the first human trial, were investigated for their ability to deliver bioavailable iron to humans in a second human study. In this study, a non-iron inhibiting food matrix (wheat bread) was used to better compare unencapsulated iron and encapsulated iron by solely focusing on absorption, as opposed to both absorption and particle-mediated protection against small molecules that chelate iron. Nine test meals containing identical doses of iron (4 mg Fe) were administered in a partially randomized single-blind, cross-over design to fasting young women [n=24, Hb: 13.2 ± 0.95 g/l, and PF: 13.2 (10.5, 16.5) µg/L] (**table S3**). Three meals contained iron as labeled ferrous sulfate in 3.19% ^{54}Fe-HA-BMC MPs, 18.29% ^{57}Fe-HA-BMC MPs, and 4 mg unencapsulated ferrous sulfate (^{58}Fe, reference meal). In all cases, iron was added prior to baking

the bread at 190°C for 20 minutes. In contrast to the first human study, 18.29% Fe-HA-BMC-MPs [FIA: 17.0 (13.2, 21.9)%] exhibited iron absorption that was not statistically different relative to unencapsulated iron [FIA: 19.2 (15.3, 24.29)%] (**Fig. 7**). The 5-fold higher loaded 3.19% Fe-HA-BMC MPs [FIA: 13.7 (11.1, 16.8)%] exhibited significant lower absorption as compared to both unencapsulated and the highest loaded 18.29% Fe-HA-BMC MPs. Compared to the reference meal, 3.19% and 18.29% Fe-HA-BMC MPs exhibited 71 (62, 82)% and 89 (74, 107)% relative iron bioavailability, respectively.

In this same human study we investigated how competitive absorption, related to the co-delivery of other micronutrients or BMC-encapsulated micronutrients alongside Fe-HA-BMC MPs, can influence absorption of iron from Fe-HA-BMC MPs. Co-delivery of VitA-BMC MPs [FIA: 12.7 (9.29, 17.5)%] or VitA-BMC MPs with free folic acid [FIA: 14.3 (11.2, 18.3)%] did not impact iron absorption **(fig. S6)**, indicating that competition between co-delivered micronutrients or BMC-encapsulated micronutrients is not a major concern for the combinations studied here. In 4 additional test meals we investigated the individual role of each MP component and how co-administering these components in free form influences absorption of iron as compared to formulation Fe-HA-BMC MPs. Our results indicated that absorption from free ferrous sulfate was not significantly affected by either HA [FIA: 20.7 (16.1, 26.7)%], BMC [FIA: 16.6 (12.0, 23.2)%], or HA-BMC [FIA: 16.3 (11.7, 22.8)%]. Similarly, when Fe was encapsulated in HA [FIA: 15.1 (11.3, 20.3)%], iron absorption was not significantly different from the reference meal. Our results indicated that absorption was not significantly affected by either HA or BMC as compared to free iron; however, when HA and BMC were formulated as MPs, a decrease in absorption compared to free iron and free iron with HA was observed **(fig. S7)**. This phenomenon is unlikely to occur for our highest loaded 18.29% Fe-HA-BMC MPs formulation, as it

demonstrated comparable absorption relative to the reference **(Fig. 7)**. Collectively, these results indicate that the absorption-limiting encapsulation that was observed in the first human study can be overcome and addressed through further development and increased loading of iron and decreased BMC content in HA-BMC MPs.

Discussion

In this work we describe polymer-based MPs that encapsulate 11 micronutrients individually or up to 4 in combination, maintain micronutrient stability during cooking and storage, and rapidly release micronutrient payloads. Modularity of the MP platform affords freedom to control the delivery and thus the dosing of each micronutrient for individual or large-population fortification needs. Studies in mice confirmed rapid micronutrient release in the stomach and absorption of vitamin A In the first human study, the bioavailability of iron from iron-loaded MPs was verified to be 44% of unencapsulated iron control after oral ingestion. Using an organotypic human intestine model, we discovered that low iron loading and high BMC amount were responsible for the lower bioavailability in this first human study. As such, process development approaches were leveraged to overcome these limitations of our lab-scale MPs. Industrially relevant spray drying and spinning disc atomization processes enabled increased iron loading while reducing the amount of BMC polymer in our iron-loaded MPs. In a subsequent human study using iron-loaded BMC MPs of over 5- and 30-fold higher iron loading and 25 and 85% less BMC polymer, we showed that our leading formulation exhibited statistically indistinguishable bioavailability as compared to an unencapsulated control. Specifically, the MP formulation of higher iron loading and lower BMC content used in the second human study address bioavailability issues; however, it should be noted that the highest iron-loaded MP exhibited lower stability in water and higher pH solutions.

As such, further optimization of BMC content and iron loading for both release and absorption may be required since variability of pH values in the stomach of human subjects at the time of ingestion (*49*) may be a potential source for observed absorption differences. Together, we describe a broad approach encompassing the design and clinical introduction of a controlled release platform for vitamins and minerals that can address unmet technological needs to improve global health.

The basis of our strategy for food fortification focused on formulation of MPs using BMC, a polymer encapsulant that has historically been used for its advantages in encapsulation, enhancing stability, facilitating rapid and controlled release, toxicity, amenability to manufacturing processes, and widespread use in many nutraceuticals and pharmaceutical products (*34-41, 50*). BMC was selected after an in-depth analysis of over fifty potential polymers. With regards to enhanced stability, it has been previously demonstrated that the water vapor permeability of BMC (*51*) is lower than what is commonly used for preservation of fruits and vegetables (*52*); thus it is likely that the known moisture barrier properties of BMC provides protection against humidity and small molecule diffusion by acting as a physical barrier between the payload and the environment. The ultraviolet-protective abilities of BMC can likely be attributed to the increased refractive index due to encapsulation in BMC (*53*), which will lower light exposure to encapsulated micronutrients. BMC is soluble at low pH in aqueous solutions and in non-aqueous solvents; as such, the solubility of BMC enabled rapid dissolution and release in stomach conditions, thus providing the versatility to facilitate encapsulation of 11 distinct micronutrients. An additional aspect of our reasoning for selecting BMC involves the existing infrastructure and knowledge-base that would enable the translation of a BMC-based technology. For example, BMC is already used commercially, has been shown to be compatible with large-

scale manufacturing processes, has a history of acceptance by the FDA, and is generally regarded as safe (*54*). The choice of solvent, DCM, used in the particle fabrication process at scale and removed afterwards, has essential roles in the preparation of other everyday consumer products such as decaffeinated coffee (*55*). Recently, the Joint Food and Agriculture Organization of the United Nations and the World Health Organization (FAO/WHO) Expert Committee on Food Additives (JECFA) yielded a positive response for BMC, specifically for micronutrient encapsulation for food fortification (*56*). JECFA concluded that the use of BMC is not a safety concern when the food additive is used for micronutrient encapsulation for food fortification at the intended use amounts and recommended an acceptable daily intake (ADI) of "not specified." Subsequently, the Codex Committee on Food Additives (CCFA) agreed to accept the JECFA recommendations (*57*). As such, concerns about the toxicity of BMC have been previously and extensively evaluated and addressed (*50, 54*); furthermore, the doses described here and the potential doses that may be used in practice would be unlikely to exceed the well-published limitations for oral exposure.

The human absorption studies described here were performed in a well-controlled setting. Both studies were performed in young healthy women where the prevalence of iron deficiency in the study population was 65 and 58% in human studies 1 and 2, respectively. The meal was specified in terms of mass and volume, the dosing of encapsulated iron was measured precisely, and the cooking conditions were well controlled using standardized procedures. Iron status will likely differ in real-world settings where people consuming the micronutrients will be from different countries where staple foods vary. Additionally, the age, health status and eating habits of individuals will vary in different cultures as well as within households. As such, further human testing for efficacy, especially in target countries and populations, will be informative for

evaluating and developing these micronutrient formulations to ensure that they are suitable in terms of stability, release, and absorption. In previous work, it has been shown that the encapsulating material can inhibit iron bioavailability (*15, 18*), which agrees with the results from both of our human studies. This relationship between the encapsulant and the micronutrient is directly tied to absorption and should be further studied for our MP platform in animals and in humans. Since micronutrients such as Vitamin A or D are more sensitive to thermal degradation as compared to iron, there exists a unique opportunity to leverage our MP platform for the storage and delivery of highly sensitive micronutrients. Our preliminary storage work and in vivo absorption work suggests that delivery of non-mineral micronutrients will be promising, however, further evidence is needed in humans. We also demonstrated successful co-encapsulation of vitamins A, D, folic acid, and B12; future efforts should focus on investigating how co-encapsulated micronutrients with known compatibility issues (*58*) may interact with each other since our study was designed to evaluate absorption of a single micronutrient (iron). The experimental approaches we have detailed here lay the groundwork to facilitate these additional studies and provide a path towards clinical translation.

In practice, translation of this technology for worldwide use, especially in countries in need of solutions for nutrition deficiencies, will still require scaling beyond the kg batch size to metric tons. Importantly, the spray drying and atomization processes described here are translatable to current commercial scale processes for micronutrients (*59*). As such, the main cost implication is directly related to the added raw material cost of BMC; future considerations to offset this cost or justify it must be considered on a country or regional level, since the severity of micronutrient deficiencies will be a driving force to balance the technical advantages offered by our encapsulation approach. Beyond manufacturing and BMC, cost considerations include the choice

of iron sulfate, since it is one of the lowest cost forms of iron (*60*) and because iron sulfate enables higher bioavailability as compared to other iron forms (*61*). Additional implications will require country-, region-, and/or individual-specific MN needs, and careful attention must be paid to local public and regulatory policies to enable widespread use of this technology. The MP delivery system has been tested in vitro, in vivo in mice, and in humans and has been scaled-up using commercially relevant processes. Furthermore, we have demonstrated the modularity and tunability of our platform by identifying and subsequently modifying the MPs to address absorption limiting design criteria. In summary, a heat-stable pH-responsive polymer-based MP delivery system has been developed that shows promise as a platform for micronutrient delivery to humans.

Materials & Methods

Study design

We hypothesized that a polymer-based MP encapsulation system that maintained micronutrient stability in boiling water for hours and rapidly releases micronutrient payloads in acidic stomach conditions could address challenges with micronutrient delivery. As such, we studied micronutrient absorption in both rodents and human subjects to evaluate our MP technology. Animal studies were approved by Institute Committee for Animal Care and Use (IACUC) and were performed at the Massachusetts Institute of Technology (MIT). For humans, two studies were performed using a single blind, randomized cross-over design. In study 1, three maize porridge test meals were administered; in study 2, participants consumed nine wheat bread test meals. All test meals were labelled with 4 mg Fe as $FeSO_4$ using stable iron isotopes (^{54}Fe, ^{57}Fe, or ^{58}Fe). Labeled $FeSO_4$ was prepared by Dr. Paul Lohmann GmbH (Germany) from isotopically ^{54}Fe- ^{58}Fe

and ^{57}Fe-enriched elemental iron (Chemgas, Boulogne, France). Particles used in study 1 were produced at MIT and those used in study 2 were produced at Southwest Research Institute (SwRI) in San Antonio, TX. Different participants were included in each study. After enrollment each participant was allocated to a predefined schedule of test meal sequence and combinations in a randomized balanced block design. Each participant served as their own control. In study 1 the maize porridge test meals contained fortified salt, added either before or after cooking. The fortified salt contained either: (a) $FeSO_4$ (reference); (b) iron-loaded BMC-HA-Fe (0.6%) added before cooking; or (c) iron-loaded BMC-HA-Fe (0.6%) added after cooking. In study 2 the wheat bread test meals were fortified before baking. The test meals contained either (a) iron-loaded BMC-HA-Fe (3.19%); (b) iron-loaded BMC-HA-Fe (18.29%); (c) iron-loaded HA-Fe (8.75%); (d) iron-loaded BMC-HA-Fe (3.19%) with VitA-BMC (3.4%; 37.65 mg vitA); (e) iron-loaded BMC-HA-Fe (3.19%) with VitA-BMC (3.4%; 37.65 mg vitA) with free folic acid (0.34 mg); (f) $FeSO_4$; (g) $FeSO_4$ with HA [25.68 mg to match HA in group (a)]; (h) FeSO4 with BMC [85.19 mg to match BMC in group (a)]; or (i) $FeSO_4$ with BMC [85.19 mg to match BMC in group (a)] with HA [25.68 mg to match HA in group (a)]. Within one week, each participant consumed a test meal on three consecutive days, and after a 14 (study 1) and 19 (study 2) day break, a blood sample was taken for measurement of stable iron isotope incorporation into the erythrocytes. In study 2 this procedure was repeated twice. The total study duration of study 1 was 17 days and study 2 was 64 days. Participants were recruited among female students at the Swiss Federal Institute of Technology in Zurich (ETH), and University of Zurich (UZH). Inclusion criteria were: apparently healthy, non-pregnant (assessed by a pregnancy test), non-lactating, age between 18 – 40 years, weight < 65 kg, body mass index (BMI) of 18.5 – 25 kg/m^2, depleted iron status defined as a plasma ferritin concentration of < 20 mg/L), and in the absence of systemic inflammation (defined

with a C-reactive protein concentration of >5 mg/L). Exclusion criteria were: chronic disease or intake of long-term medication (except for oral contraceptives), consumption of mineral and vitamin supplements within the 2 weeks before 1st test meal administration; and significant blood loss or transfusion, within 4 months before the study initiation. Informed written consent was obtained from all participants. Ethical approval for both studies were provided by the ethical review committee of Cantonal Ethics Commission of Zurich (study 1: KEK-ZH-Nr. 2015-0094; study 2: KEK-ZH-Nr. 2017-01624) and the Committee on the Use of Humans as Experimental Subjects at MIT (study 1: COUHES # 1502006932; study 2: COUHES # 1801201448/1801201448A001); both trials were registered on ClinicalTrials.gov: study 1 (NCT02353325) and study 2 (NCT03332602). Both studies were powered to detect a nutritionally relevant, 30% within-group difference in iron absorption, based on a standard deviation of 0.35 from log transformed iron absorption from previous studies by our laboratory (*62*), an α level of 5% (two tailed) and 80% power; 18 subjects were calculated. In study 1 a 10% drop-out rate was anticipated; in study 2, due to the longer duration of the study a 30% drop-out rate was anticipated, therefore 20 and 24 subjects were recruited, respectively.

Formulation of one-step MPs (BMC MPs) and two-step MPs (HA-BMC MPs)

BMC MPs were prepared by a modified oil/water emulsion method (*63*). The organic phase for the emulsion consisted of either: (a) one milligram of blank, or dye labelled HA MPs homogeneously dispersed in 1 ml of 100 mg/ml BMC solution in methylene chloride; (b) vitamin A (10 mg/ml), vitamin D (2 mg/ml), folic acid-loaded HA MPs (1.3 mg), and B12-loaded HA MPs (1.3 mg) dissolved into BMC solution (100 mg/ml, 1ml) in methylene chloride to prepare BMC MPs co-encapsulated with four different types of micronutrients; (c) HA MPs encapsulated with

various micronutrients as described in **table S2** to synthesize HA-BMC MPs with various micronutrient loads; (d), free micronutrients as described in **table S2** to synthesize BMC MPs with various micronutrient loads; or (e) 1 mg/ml lipophilic carbocyanine DiOC18(7) dye (DiR, Life Technologies) and 100 mg/ml BMC in methylene chloride to synthesize fluorescently labeled BMC MPs. The resulting organic phases were then emulsified in 20 ml, 10 mg/ml polyvinyl alcohol (PVA) solution with a stirring rate at 300 rpm for 10 min. The obtained emulsion was added into 100 ml de-ionized water with stirring (500 rpm for 10 min) to solidify the MPs. The obtained MPs were allowed to settle by gravity and were thoroughly washed with water. The final dry MPs were obtained by lyophilization.

Micronutrient-MP loading, release, and stability

Vitamins B2, Niacin, Folic acid, B12, A, and D were analyzed via High performance liquid chromatography (HPLC, Agilent 1100; Agilent Technologies) using a C-18 column (Acclaim PolarAdvantage II, 3 μm, 4.6 × 150 mm) and were detected by a photodiode detector at 265, 265, 286, 550, 325, and 264 nm, respectively. Iron, biotin, zinc, and vitamin C were analyzed via BioVision colorimetric assay kits and vitamin biotin was analyzed via a Sigma colorimetric assay kit. Iodine was measured using UV-Vis absorbance at 288 nm. DiR-loaded BMC MPs were dissolved in DMSO, and then the dissolved cargo was quantified using a multimode reader (TECAN InfiniteM200 PRO) at 750nm. Micronutrient-loaded HA MPs were dissolved in water, and micronutrient content was determined as described above for each respective micronutrient. To quantify micronutrient loading in the co-encapsulated HA-BMC MPs or the BMC MPs, a known mass of MPs was first dissolved in SGF and then analyzed for total micronutrient mass. The precipitated BMC was removed via centrifugation using Amicon Ultra centrifuge filters (3000

NMWL) at 14000 x g for 30 min to remove HA and BMC. The dissolved micronutrients were separated and quantified as described above. To quantify vitamins A and D loading, the MPs were dissolved in methylene chloride and the dissolved vitamins A and D were separated and quantified as described above. The release profiles of micronutrients were studied in water at RT, boiling water at 100°C, and SGF at 37°C. At each time point, samples were centrifuged at 4000 rpm for 5 min and 900 µl of the supernatant was collected for analysis, and then samples were replenished with 900 µl of fresh release medium. For vitamins A and D, the aqueous release medium was brought into contact with a layer of methylene chloride, then the extracted fat-soluble vitamins within the organic phase were used for analysis. The cumulative release was calculated as the total amount of micronutrient released at a particular time point relative to the amount initially loaded. Dry micronutrients were dispersed in water and then heated at 100°C for 2 hours before being centrifuged at 4000 rpm for 5 min. The stability percentage equals the ratio of stable micronutrient after to the actual loading of the micronutrient in the MPs. For samples in unencapsulated form, they were either dissolved in water or dispersed in water before being heated for 2 hrs. The sensory performance was measured in duplicate as the absolute color change in a food matrix after the addition of the Fe microspheres. A banana-milk slurry was chosen as polyphenol rich food matrix. The fortificants were added to 70 g banana-milk at a concentration of 60 ppm Fe in banana milk. The banana milk was prepared fresh 180 g fresh banana with 520 g organic whole milk (3.9% fat, homogenized, pasteurized). Color change was measured in duplicate at baseline (before fortification) and 2 hours after fortification and stirring at 350 rpm. The absolute color change of ΔE was measured and calculated as previously described (*64*). $FeSO_4$ and ferric pyrophosphate (FePP, 20% Fe, micronized powder) were used as positive and negative controls.

Dissolution study of DiR-loaded BMC MPs in mice

Female SKH1-Elite mice (Crl:SKH1-hr) were purchased from Charles River Laboratories at 8-12 weeks of age. Mice were fed an alfalfa-free balanced diet (Harlan Laboratories, AIN-76A) for 10 days prior to treatment to reduce food-related autofluorescence. About 200 mg of DiR-loaded BMC MPs was administered in 100 µl of water via gavage (n=3). After 15, 30, or 60 minutes, mice were euthanized using carbon dioxide asphyxiation. The gastrointestinal tract was immediately explanted and imaged using In Vivo Imaging System (IVIS, PerkinElmer). The fluorescent signals from mice that had ingested DiR-loaded BMC MPs were compared to mice that did not receive MPs. The spectral signatures associated with encapsulated and released DiR were then computationally separated from tissue autofluorescence (identified in the control samples) to determine the location and status of dye release. Quantified signal/background ratios were determined by normalizing the encapsulated or released dye signal, in either the stomach or intestines, to a background in control animals receiving no BMC MPs.

In vivo vitamin A absorption in rats

Tritium-labeled retinyl palmitate (American Radiolabeled Chemicals, Inc.), was used to detect the amount of absorbed vitamin A in blood. Radiolabeled VitA-BMC MPs were prepared by the O/W emulsion method described above. Female Wistar rats (~250g) were purchased from Charles River Laboratories. The rats were divided into two groups: (i) free vitamin A and (ii) VitA-BMC MPs. In the free group, vitamin A was delivered in a 4% v/v ethanol/water mixture to enable solubilization of vitamin A. The VitA-BMC MPs were dispersed in water and vortexed to form a suspension. Each rat was oral gavaged 10 µCi of vitamin A in either its free form or encapsulated MPs in 350 µL of either ethanol/water mixture or water total. Residual vitamin A in the syringe

and gavage needle were saved and quantified by scintillation counter to calculate the actual feeding amount of T-RP for each rat. At 0.5, 1, 2, 3, 4, 5, 6 hours, the rats were anesthetized via isoflurane and 200 μL of blood were collected from lateral tail vein. The radioactivity in the samples were quantified vita liquid scintillation counting with a Tri-Carb 2810 TR liquid scintillation counter. To calculate loading of vitamin A in the VitA-BMC MPs, the MPs were first dissolved in 1 mL dichloromethane, and then 5 μL of the solution was mixed with 10 mL Ultima Gold F liquid scintillation cocktail (PerkinElmer Inc.). Blood (200 μL) was dissolved in SOLVABLE (PerkinElmer Inc.) following recommended protocol, and then 1 mL of the dissolved blood was mixed with 10 mL Hionic-Fluor liquid scintillation cocktail.

MatTek EpiIntestinal transport

EpiIntestinal tissues were purchased from MatTek (Ashland) and used as recommended. For transport experiments, the particle constituents BMC, Fe, and HA were separately prepared and added to achieve final mass percentages as reported. After 1 hour of incubation at 37°C and 5% CO_2, transport iron was analyzed in the bottom transwell chamber using the previously described BioVision colorimetric assay.

Process development and scale-up

The detailed process described here was used to manufacture 1 kg of Fe-HA-BMC MPs as shown in **Fig. 6**. A Niro Production Minor pilot scale spray dryer was used to first prepare Fe-HA MPs. The feed solution contained 525.5 g sodium hyaluronate, 1309.5 g iron sulfate monohydrate, and 77 L of deionized water. This solution was fed into the dryer at 250 g/min and atomized with a 2 mm two-fluid nozzle. The dryer inlet temperature was set to 257°C, resulting in an outlet

temperature of 90°C. 1215 g of MPs was recovered. Fe-HA MPs were encapsulated with BMC using a custom spinning disc atomization system. The feed solution was prepared with 1152 g of BMC and 1.87 g of polysorbate 80 dissolved in 12000 g of dichloromethane (DCM). 48 g of Fe-HA MPs was added to the DCM solution and placed in a sonication bath for 10 minutes to form a stable suspension. The suspension was fed at 110 g/min onto a 10.16-cm diameter stainless steel custom disc spinning at 1300 rpm. The disc was mounted 9.144 m high in a 6.096 m × 6.096 m tower. The room was heated to 35-40°C. Particles were collected on antistatic plastic located at the bottom of the tower. 1059 g of MPs were recovered. These processes were modified for batches used in human study 2 by using a Pro-CepT 4M8 laboratory spray dryer for the Fe-HA MPs. All new tubing and filters were used with the spray dryer, in addition to cleaning all wetted parts with soapy water and a 70% aqueous isopropanol (IPA) solution. The inlet temperature for the spray dryer was set to 160°C, resulting in an outlet temperature of approximately 53°C. Solution was dried at 8 mL/min through a 0.4 mm air atomized nozzle. The same spinning disc setup was used for encapsulating the Fe-HA MPs within BMC. The tower was mopped and cleaned, followed by treatment with Vesphene IIse. Encapsulated Vitamin A for feed studies was also prepared using the same spinning disc system. A disc speed of 1675 rpm was used as the feed solution was fed to a 10.16-cm spinning disc at approximately 115 g/min. The material was collected in a powdered by of DryFlo starch. The excess starch was then sieved from the sample to recover the Vitamin A MPs. All samples were placed under vacuum with a slow N_2 purge for 1 week to remove residual DCM. Specific feed conditions for the MPs used in human study 2 are listed in **table S4**.

Statistical analysis

For in vitro and rodent studies, all quantitative measurements were performed on three independent replicates. All values are expressed as means ± standard deviations (SD). Statistical significance was evaluated using a two-tailed Student's t-test. Statistical analysis of the human studies were done using SPSS Version 22 (human study 1) and Version 24 (human study 2) (IBM SPSS Statistics). All data were checked for normal distribution before analysis: Age, weight, height, Hb, CRP were normal and the data are presented as means and standard deviations (SD). PF and fractional Fe absorption are non-normal and are presented as geometric means and 95% confidence interval (CI). Comparisons between meals were done using the square root transformed data fitted in a linear mixed model. Meals were entered as a repeated fixed factor (covariance type of scaled identity) and subjects as random factors (intercept). If a significant overall effect of meals was found, post-hoc tests within different meals were performed using the Bonferroni correction for multiple comparisons. A P value of < 0.05 was considered statistically different.

List of Supplementary Materials

Fig. S7. Comparison of iron absorption from 3.19% Fe-HA-BMC MPs with each MP constituent both individually and in combination

Table S1. Polymers evaluated as potential MP matrix materials

Table S2: Formulation parameters and loadings for lab-scale microparticles

Table S3. Subject characteristics of human study 1 and 2

Table S4. Process design formulation parameters and loadings for MPs used in the second human study

Table S5. Quality control tests for MPs used in both human studies

References

1. K. M. Jamil, A. S. Rahman, P. Bardhan, A. I. Khan, F. Chowdhury, S. A. Sarker, A. M. Khan, T. Ahmed, Micronutrients and anaemia. *Journal of health, population, and nutrition* **26**, 340 (2008).
2. S. S. Lim, T. Vos, A. D. Flaxman, G. Danaei, K. Shibuya, H. Adair-Rohani, M. Amann, H. R. Anderson, K. G. Andrews, M. Aryee, C. Atkinson, L. J. Bacchus, A. N. Bahalim, K. Balakrishnan, J. Balmes, S. Barker-Collo, A. Baxter, M. L. Bell, J. D. Blore, F. Blyth, C. Bonner, G. Borges, R. Bourne, M. Boussinesq, M. Brauer, P. Brooks, N. G. Bruce, B. Brunekreef, C. Bryan-Hancock, C. Bucello, R. Buchbinder, F. Bull, R. T. Burnett, T. E. Byers, B. Calabria, J. Carapetis, E. Carnahan, Z. Chafe, F. Charlson, H. Chen, J. S. Chen, A. T. Cheng, J. C. Child, A. Cohen, K. E. Colson, B. C. Cowie, S. Darby, S. Darling, A. Davis, L. Degenhardt, F. Dentener, D. C. Des Jarlais, K. Devries, M. Dherani, E. L. Ding, E. R. Dorsey, T. Driscoll, K. Edmond, S. E. Ali, R. E. Engell, P. J. Erwin, S. Fahimi, G. Falder, F. Farzadfar, A. Ferrari, M. M. Finucane, S. Flaxman, F. G. Fowkes, G. Freedman, M. K. Freeman, E. Gakidou, S. Ghosh, E. Giovannucci, G. Gmel, K. Graham, R. Grainger, B. Grant, D. Gunnell, H. R. Gutierrez, W. Hall, H. W. Hoek, A. Hogan, H. D. Hosgood, 3rd, D. Hoy, H. Hu, B. J. Hubbell, S. J. Hutchings, S. E. Ibeanusi, G. L. Jacklyn, R. Jasrasaria, J. B. Jonas, H. Kan, J. A. Kanis, N. Kassebaum, N. Kawakami, Y. H. Khang, S. Khatibzadeh, J. P. Khoo, C. Kok, F. Laden, R. Lalloo, Q. Lan, T. Lathlean, J. L. Leasher, J. Leigh, Y. Li, J. K. Lin, S. E. Lipshultz, S. London, R. Lozano, Y. Lu, J. Mak, R. Malekzadeh, L. Mallinger, W. Marcenes, L. March, R. Marks, R. Martin, P. McGale, J. McGrath, S. Mehta, G. A. Mensah, T. R. Merriman, R. Micha, C. Michaud, V. Mishra, K. Mohd Hanafiah, A. A. Mokdad, L. Morawska, D. Mozaffarian, T. Murphy, M. Naghavi, B. Neal, P. K. Nelson, J. M. Nolla, R. Norman, C. Olives, S. B. Omer, J. Orchard, R. Osborne, B. Ostro, A. Page, K. D. Pandey, C. D. Parry, E. Passmore, J. Patra, N. Pearce, P. M. Pelizzari, M. Petzold, M. R. Phillips, D. Pope, C. A. Pope, 3rd, J. Powles, M. Rao, H. Razavi, E. A. Rehfuess, J. T. Rehm, B. Ritz, F. P. Rivara, T. Roberts, C. Robinson, J.

A. Rodriguez-Portales, I. Romieu, R. Room, L. C. Rosenfeld, A. Roy, L. Rushton, J. A. Salomon, U. Sampson, L. Sanchez-Riera, E. Sanman, A. Sapkota, S. Seedat, P. Shi, K. Shield, R. Shivakoti, G. M. Singh, D. A. Sleet, E. Smith, K. R. Smith, N. J. Stapelberg, K. Steenland, H. Stockl, L. J. Stovner, K. Straif, L. Straney, G. D. Thurston, J. H. Tran, R. Van Dingenen, A. van Donkelaar, J. L. Veerman, L. Vijayakumar, R. Weintraub, M. M. Weissman, R. A. White, H. Whiteford, S. T. Wiersma, J. D. Wilkinson, H. C. Williams, W. Williams, N. Wilson, A. D. Woolf, P. Yip, J. M. Zielinski, A. D. Lopez, C. J. Murray, M. Ezzati, M. A. AlMazroa, Z. A. Memish, A comparative risk assessment of burden of disease and injury attributable to 67 risk factors and risk factor clusters in 21 regions, 1990-2010: a systematic analysis for the Global Burden of Disease Study 2010. *Lancet (London, England)* **380**, 2224-2260 (2012).

3. M. B. Zimmermann, P. L. Jooste, C. S. Pandav, Iodine-deficiency disorders. *The Lancet* **372**, 1251-1262 (2008).
4. F. A. Oski, Iron deficiency in infancy and childhood. *The New England journal of medicine* **329**, 190-193 (1993).
5. E. M. Wiseman, S. Bar-El Dadon, R. Reifen, The vicious cycle of vitamin A deficiency: A review. *Critical reviews in food science and nutrition*, 0 (2016).
6. D. O. Kennedy, B vitamins and the brain: Mechanisms, dose and efficacy—A review. *Nutrients* **8**, 68 (2016).
7. N. E. Palermo, M. F. Holick, Vitamin D, bone health, and other health benefits in pediatric patients. *Journal of Pediatric Rehabilitation Medicine: An Inderdisciplinary Approach* **7**, (2014).
8. R. Black, Micronutrient deficiency: an underlying cause of morbidity and mortality. *Bulletin of the World Health Organization* **81**, 79-79 (2003).
9. F. J. Levinson, L. Bassett, Malnutrition is still a major contributor to child deaths. *Population Reference Bureau*, (2007).
10. Z. A. Bhutta, R. A. Salam, Global nutrition epidemiology and trends. *Annals of Nutrition and Metabolism* **61**, 19-27 (2013).
11. A. M. Leung, L. E. Braverman, E. N. Pearce, History of US iodine fortification and supplementation. *Nutrients* **4**, 1740-1746 (2012).
12. K. Charlton, S. Skeaff, Iodine fortification: why, when, what, how, and who? *Current Opinion in Clinical Nutrition & Metabolic Care* **14**, 618-624 (2011).
13. G. Arroyave, L. A. Mejia, J. R. Aguilar, The effect of vitamin A fortification of sugar on the serum vitamin A levels of preschool Guatemalan children: a longitudinal evaluation. *The American journal of clinical nutrition* **34**, 41-49 (1981).
14. C. Liyanage, S. Zlotkin, Bioavailability of iron from micro-encapsulated iron sprinkle supplement. *Food and nutrition bulletin* **23**, 133-137 (2002).
15. M. B. Zimmermann, The potential of encapsulated iron compounds in food fortification: A review. *Int J Vitam Nutr Res* **74**, 453-461 (2004).
16. I. Raileanu, L. L. Diosady, Vitamin A stability in salt triple fortified with iodine, iron, and vitamin A. *Food and nutrition bulletin* **27**, 252-259 (2006).
17. P. Sauvant, M. Cansell, A. Hadj Sassi, C. Atgié, Vitamin A enrichment: Caution with encapsulation strategies used for food applications. *Food Research International* **46**, 469–479 (2012).

18. D. Moretti, M. Zimmermann, Assessing bioavailability and nutritional value of microencapsulated minerals. *Encapsulation and Controlled Release Technologies in Food Systems*, 289 (2016).
19. R. L. Bailey, K. P. West Jr, R. E. Black, The epidemiology of global micronutrient deficiencies. *Annals of Nutrition and Metabolism* **66**, 22-33 (2015).
20. M. Andersson, V. Karumbunathan, M. B. Zimmermann, Global iodine status in 2011 and trends over the past decade. *The Journal of nutrition* **142**, 744-750 (2012).
21. R. E. Black, in *International Nutrition: Achieving Millennium Goals and Beyond*. (Karger Publishers, 2014), vol. 78, pp. 21-28.
22. L. H. Allen, in *Hidden Hunger*. (Karger Publishers, 2016), vol. 115, pp. 109-117.
23. F. E. Runge, R. Heger, Use of microcalorimetry in monitoring stability studies. Example: vitamin A esters. *Journal of agricultural and food chemistry* **48**, 47-55 (2000).
24. I. Van den Broeck, L. Ludikhuyze, C. Weemaes, A. Van Loey, M. Hendrickx, Kinetics for isobaric-isothermal degradation of L-ascorbic acid. *Journal of agricultural and food chemistry* **46**, 2001-2006 (1998).
25. M. Allwood, J. Plane, The wavelength-dependent degradation of vitamin A exposed to ultraviolet radiation. *International journal of pharmaceutics* **31**, 1-7 (1986).
26. C. V. Moore, R. Dubach, V. Minnich, H. K. Roberts, Absorption of ferrous and ferric radioactive iron by human subjects and by dogs. *Journal of Clinical Investigation* **23**, 755 (1944).
27. H. Kwak, K. Yang, J. Ahn, Microencapsulated iron for milk fortification. *Journal of agricultural and food chemistry* **51**, 7770-7774 (2003).
28. D. J. McClements, E. A. Decker, J. Weiss, Emulsion-based delivery systems for lipophilic bioactive components. *Journal of food science* **72**, R109-R124 (2007).
29. Y. O. Li, L. L. Diosady, A. S. Wesley, Folic Acid Fortification through Existing Fortified Foods: Iodized Salt and Vitamin A—Fortified Sugar. *Food and nutrition bulletin* **32**, 35-41 (2011).
30. D. J. McClements, Nanoscale nutrient delivery systems for food applications: improving bioactive dispersibility, stability, and bioavailability. *Journal of food science* **80**, N1602-N1611 (2015).
31. R. Y. Yada, N. Buck, R. Canady, C. DeMerlis, T. Duncan, G. Janer, L. Juneja, M. Lin, D. J. McClements, G. Noonan, Engineered nanoscale food ingredients: evaluation of current knowledge on material characteristics relevant to uptake from the gastrointestinal tract. *Comprehensive Reviews in Food Science and Food Safety* **13**, 730-744 (2014).
32. J. Yi, Y. Fan, W. Yokoyama, Y. Zhang, L. Zhao, Thermal Degradation and Isomerization of β-Carotene in Oil-in-Water Nanoemulsions Supplemented with Natural Antioxidants. *Journal of agricultural and food chemistry* **64**, 1970-1976 (2016).
33. Y. O. Li, D. Yadava, K. L. Lo, L. L. Diosady, A. S. Wesley, Feasibility and optimization study of using cold-forming extrusion process for agglomerating and microencapsulating ferrous fumarate for salt double fortification with iodine and iron. *Journal of microencapsulation* **28**, 639-649 (2011).
34. M. Bogataj, A. Mrhar, A. Kristl, F. Kozjek, Preparation and evaluation of Eudragit E microspheres containing bacampicillin. *Drug Development and Industrial Pharmacy* **15**, 2295-2313 (1989).

35. M. Lorenzo-Lamosam, M. Cuñaj, L. Vila-Jatod, D. Torres, M. Alonso, Development of a microencapsulated form of cefuroxime axetil using pH-sensitive acrylic polymers. *Journal of microencapsulation* **14**, 607-616 (1997).
36. R. Schellekens, F. Stellaard, D. Mitrovic, F. Stuurman, J. Kosterink, H. Frijlink, Pulsatile drug delivery to ileo-colonic segments by structured incorporation of disintegrants in pH-responsive polymer coatings. *Journal of controlled release* **132**, 91-98 (2008).
37. R. Mustafin, Interpolymer combinations of chemically complementary grades of Eudragit copolymers: a new direction in the design of peroral solid dosage forms of drug delivery systems with controlled release (review). *Pharmaceutical Chemistry Journal* **45**, 285-295 (2011).
38. R. Moustafine, A. Bukhovets, A. Sitenkov, V. Kemenova, P. Rombaut, G. Van den Mooter, Eudragit E PO as a complementary material for designing oral drug delivery systems with controlled release properties: comparative evaluation of new interpolyelectrolyte complexes with countercharged eudragit L100 copolymers. *Molecular pharmaceutics* **10**, 2630-2641 (2013).
39. B. Karolewicz, A review of polymers as multifunctional excipients in drug dosage form technology. *Saudi Pharmaceutical Journal*, (2015).
40. J. Eisele, G. Haynes, K. Kreuzer, C. Hall, Toxicological assessment of Anionic Methacrylate Copolymer: I. Characterization, bioavailability and genotoxicity. *Regulatory toxicology and pharmacology : RTP* **82**, 39-47 (2016).
41. P. Li, Z. Yang, Y. Wang, Z. Peng, S. Li, L. Kong, Q. Wang, Microencapsulation of coupled folate and chitosan nanoparticles for targeted delivery of combination drugs to colon. *Journal of microencapsulation* **32**, 40-45 (2015).
42. M. Haham, S. Ish-Shalom, M. Nodelman, I. Duek, E. Segal, M. Kustanovich, Y. D. Livney, Stability and bioavailability of vitamin D nanoencapsulated in casein micelles. *Food & function* **3**, 737-744 (2012).
43. R. I. Mellican, J. Li, H. Mehansho, S. S. Nielsen, The role of iron and the factors affecting off-color development of polyphenols. *Journal of agricultural and food chemistry* **51**, 2304-2316 (2003).
44. C. Z. Ran, A. Moore, Spectral Unmixing Imaging of Wavelength-Responsive Fluorescent Probes: An Application for the Real-Time Report of Amyloid Beta Species in Alzheimer's Disease. *Molecular Imaging and Biology* **14**, 293-300 (2012).
45. L. Hallberg, M. Brune, L. Rossander, Iron absorption in man: ascorbic acid and dose-dependent inhibition by phytate. *The American journal of clinical nutrition* **49**, 140-144 (1989).
46. I. Maschmeyer, T. Hasenberg, A. Jaenicke, M. Lindner, A. K. Lorenz, J. Zech, L. A. Garbe, F. Sonntag, P. Hayden, S. Ayehunie, R. Lauster, U. Marx, E. M. Materne, Chip-based human liver-intestine and liver-skin co-cultures--A first step toward systemic repeated dose substance testing in vitro. *Eur J Pharm Biopharm* **95**, 77-87 (2015).
47. J. P. Wikswo, The relevance and potential roles of microphysiological systems in biology and medicine. *Exp Biol Med (Maywood)* **239**, 1061-1072 (2014).
48. C. P. Reis, R. J. Neufeld, A. J. Ribeiro, F. Veiga, Nanoencapsulation I. Methods for preparation of drug-loaded polymeric nanoparticles. *Nanomedicine: Nanotechnology, Biology and Medicine* **2**, 8-21 (2006).

49. J. B. Dressman, R. R. Berardi, L. C. Dermentzoglou, T. L. Russell, S. P. Schmaltz, J. L. Barnett, K. M. Jarvenpaa, Upper gastrointestinal (GI) pH in young, healthy men and women. *Pharmaceutical research* **7**, 756-761 (1990).
50. S. Thakral, N. K. Thakral, D. K. Majumdar, Eudragit®: a technology evaluation. *Expert opinion on drug delivery* **10**, 131-149 (2013).
51. D. Klimkowsky, Moisture Protection and Taste-Masking with Polymethacrylate Coatings [powerpoint slides]. *Evonik Industries: 2008.* **Available from: http://www.phexcom.cn/uploadfiles/200899112713336.pdf.**
52. A. A. Kader, D. Zagory, E. L. Kerbel, C. Y. Wang, Modified atmosphere packaging of fruits and vegetables. *Critical Reviews in Food Science & Nutrition* **28**, 1-30 (1989).
53. E.-C. Cho, Effect of polymer characteristics on the thermal stability of retinol encapsulated in aliphatic polyester nanoparticles. *Bulletin of the Korean Chemical Society* **33**, 2560-2566 (2012).
54. J. Eisele, G. Haynes, T. Rosamilia, Characterisation and toxicological behaviour of basic methacrylate copolymer for GRAS evaluation. *Regulatory Toxicology and Pharmacology* **61**, 32-43 (2011).
55. K. Ramalakshmi, B. Raghavan, Caffeine in coffee: its removal. Why and how? *Critical reviews in food science and nutrition* **39**, 441-456 (1999).
56. *Joint FAO/WHO Expert Committee on Food Additives, Summary and Conclusions, 86th meeting, Geneva, June 12-21, 2018* Available from: http://www.fao.org/fileadmin/user_upload/agns/pdf/jecfa/JECFA86_Summary_Report.pdf, Accessed 10/28/2018.
57. *Report of the 51st Session of the Codex Committee on Food Additives, Jinan, China, March 25-29, 2019*. Available from: http://www.fao.org/fao-who-codexalimentarius/sh-proxy/en/?lnk=1&url=https%253A%252F%252Fworkspace.fao.org%252Fsites%252Fcodex%252FMeetings%252FCX-711-51%252FReport%252FREP19_FAe.pdf, Accessed 05/27/2019.
58. B. Sandström, Micronutrient interactions: effects on absorption and bioavailability. *British journal of Nutrition* **85**, S181-S185 (2001).
59. R. Murugesan, V. Orsat, Spray drying for the production of nutraceutical ingredients—a review. *Food and Bioprocess Technology* **5**, 3-14 (2012).
60. O. Schröder, O. Mickisch, U. Seidler, A. De Weerth, A. U. Dignass, H. Herfarth, M. Reinshagen, S. Schreiber, U. Junge, M. Schrott, J. Stein, Intravenous iron sucrose versus oral iron supplementation for the treatment of iron deficiency anemia in patients with inflammatory bowel disease—a randomized, controlled, open-label, multicenter study. *The American journal of gastroenterology* **100**, 2503 (2005).
61. A. B. Pérez-Expósito, S. Villalpando, J. A. Rivera, I. J. Griffin, S. A. Abrams, Ferrous sulfate is more bioavailable among preschoolers than other forms of iron in a milk-based weaning food distributed by PROGRESA, a national program in Mexico. *The Journal of nutrition* **135**, 64-69 (2005).
62. I. Herter-Aeberli, K. Eliancy, Y. Rathon, C. U. Loechl, J. M. Pierre, M. B. Zimmermann, In Haitian women and preschool children, iron absorption from wheat flour-based meals fortified with sodium iron EDTA is higher than that from meals fortified with ferrous fumarate, and is not affected by Helicobacter pylori infection in children. *British Journal of Nutrition* **118**, 273-279 (2017).

63. T. Kemala, E. Budianto, B. Soegiyono, Preparation and characterization of microspheres based on blend of poly(lactic acid) and poly(epsilon-caprolactone) with poly(vinyl alcohol) as emulsifier. *Arabian Journal of Chemistry* **5**, 103-108 (2012).
64. Y. Shen, L. Posavec, S. Bolisetty, F. M. Hilty, G. Nystrom, J. Kohlbrecher, M. Hilbe, A. Rossi, J. Baumgartner, M. B. Zimmermann, R. Mezzenga, Amyloid fibril systems reduce, stabilize and deliver bioavailable nanosized iron. *Nat Nanotechnol* **12**, 642-647 (2017).
65. A. K. Jha, X. A. Xu, R. L. Duncan, X. Q. Jia, Controlling the adhesion and differentiation of mesenchymal stem cells using hyaluronic acid-based, doubly crosslinked networks. *Biomaterials* **32**, 2466-2478 (2011).
66. X. Q. Jia, Y. Yeo, R. J. Clifton, T. Jiao, D. S. Kohane, J. B. Kobler, S. M. Zeitels, R. Langer, Hyaluronic acid-based microgels and microgel networks for vocal fold regeneration. *Biomacromolecules* **7**, 3336-3344 (2006).
67. A. K. Jha, R. A. Hule, T. Jiao, S. S. Teller, R. J. Clifton, R. L. Duncan, D. J. Pochan, X. Q. Jia, Structural Analysis and Mechanical Characterization of Hyaluronic Acid-Based Doubly Cross-Linked Networks. *Macromolecules* **42**, 537-546 (2009).
68. R. U. Makower, Extraction and Determination of Phytic Acid in Beans (Phaseolus-Vulgaris). *Cereal Chem* **47**, 288-& (1970).
69. World Health Organization. Dept. of Nutrition for Health and Development., *Iron deficiency anaemia : assessment, prevention and control : a guide for programme managers*. (World Health Organization, Geneva, 2001), pp. 114 p.
70. C. I. Cercamondi, I. M. Egli, E. Mitchikpe, F. Tossou, C. Zeder, J. D. Hounhouigan, R. F. Hurrell, Total iron absorption by young women from iron-biofortified pearl millet composite meals is double that from regular millet meals but less than that from post-harvest iron-fortified millet meals. *J Nutr* **143**, 1376-1382 (2013).
71. E. Brown, B. Bradley, R. Wennesland, J. L. Hodges, J. Hopper, H. Yamauchi, Red Cell, Plasma, and Blood Volume in Healthy Women Measured by Radichromium Cell-Labeling and Hematocrit. *J Clin Invest* **41**, 2182-& (1962).
72. V. Kumar, T. Yang, Y. Yang, Interpolymer complexation. I. Preparation and characterization of a polyvinyl acetate phthalate-polyvinylpyrrolidone (PVAP-PVP) complex. *International journal of pharmaceutics* **188**, 221-232 (1999).
73. Colorcon. *OPADRY® Enteric: Acrylic-Based Coating System – 91 Series*. 2013; Available from: https://www.colorcon.com/literature/marketing/mr/Delayed%20Release/Opadry%20Enteric/Chinese/product_info.pdf.
74. Eastman. *Eastman C-A-P enteric coating materials (Cellulose acetate phthalate or cellacefate, NF)*. 2016; Available from: http://www.eastman.com/Literature_Center/C/CECOAT3143.pdf.
75. P. Roxin, A. Karlsson, S. K. Singh, Characterization of cellulose acetate phthalate (CAP). *Drug development and industrial pharmacy* **24**, 1025-1041 (1998).
76. C. Malm, J. Emerson, G. Hiait, Cellulose acetate phthalate as an enteric coating material. *Journal of the American Pharmaceutical Association* **40**, 520-525 (1951).
77. ShinEtsu. *USP Hypromellose Phthalate HPMCP*. 2002; Available from: http://www.metolose.ru/files/hpmcp.pdf.
78. K. Thoma, K. Bechtold, Influence of aqueous coatings on the stability of enteric coated pellets and tablets. *European journal of pharmaceutics and biopharmaceutics* **47**, 39-50 (1999).

79. ShinEtsu. *Hypromellose Acetate Succinate: Shin-Etsu AQOAT*. 2005; Available from: http://www.elementoorganika.ru/files/aqoat.
80. Z. Dong, D. S. Choi, Hydroxypropyl methylcellulose acetate succinate: Potential drug–excipient incompatibility. *AAPs Pharmscitech* **9**, 991-997 (2008).
81. Swadeshi International Company. *Dewaxed Decolourised Shellac (Flakes)*. Available from: Available from: http://www.shellac.in/shellac_machinemade.html.
82. Y. Farag, C. Leopold, Physicochemical properties of various shellac types. *Dissolut Technol* **16**, 33-39 (2009).
83. S. Limmatvapirat, C. Limmatvapirat, S. Puttipipatkhachorn, J. Nuntanid, M. Luangtana-anan, Enhanced enteric properties and stability of shellac films through composite salts formation. *European Journal of Pharmaceutics and Biopharmaceutics* **67**, 690-698 (2007).
84. A. Patel, P. Heussen, J. Hazekamp, K. P. Velikov, Stabilisation and controlled release of silibinin from pH responsive shellac colloidal particles. *Soft Matter* **7**, 8549-8555 (2011).
85. M. L. Aldridge. *Re: Docket No. 02N-0434 Withdrawal of Certain Proposed Rules and Other Proposed Actions; Notice of Intent*. 2003; Available from: https://www.fda.gov/ohrms/dockets/dailys/03/jul03/072803/02n-0434-c000017-vol3.pdf.
86. Kitozyme. *Chitosan GRAS Notice*. 2011; Available from: https://www.fda.gov/downloads/Food/IngredientsPackagingLabeling/GRAS/NoticeInventory/ucm277279.pdf.
87. C. Qin, H. Li, Q. Xiao, Y. Liu, J. Zhu, Y. Du, Water-solubility of chitosan and its antimicrobial activity. *Carbohydrate polymers* **63**, 367-374 (2006).
88. E. Szymańska, K. Winnicka, Stability of chitosan—a challenge for pharmaceutical and biomedical applications. *Marine drugs* **13**, 1819-1846 (2015).
89. Evonik. *Eudragit® polymers – defining targeted drug release*. Available from: http://healthcare.evonik.com/sites/lists/NC/DocumentsHC/Evonik-Eudragit_brochure.pdf.
90. C. N. Patra, R. Priya, S. Swain, G. K. Jena, K. C. Panigrahi, D. Ghose, Pharmaceutical significance of Eudragit: A review. *Future Journal of Pharmaceutical Sciences*, (2017).
91. Evonik. *Advanced functional coating solutions for nutraceuticals*. Available from: http://healthcare.evonik.com/sites/lists/NC/DocumentsHC/Evonik_EUDRAGUARD%20nutritional%20coating%20solutions_brochure.pdf.
92. Evonik. *EUDRAGIT® E 100, EUDRAGIT® E PO and EUDRAGIT® E 12,5*. 2015; Available from: https://www.pharma-excipients.ch/app/download/10453336098/TI-EUDRAGIT-E-100-E-PO-E-12-5-EN.pdf?t=1459521322.

Acknowledgements: We acknowledge W. H. Gates, S. Kern, K. Owen, L. Shackelton, C. Karp, D. Hartman, and S. Hershenson, K. Brown, S. Torgerson, and S. Baker, for their advice and guidance. **Funding:** This work was funded by the Bill & Melinda Gates Foundation OPP1087261.

Author contributions: A.C.A., X.X., B.N., L.W., P.A.W., J.D.O., D.M., M.B.Z., R.L., and A.J. conceived and designed the research. X.X., J.D.O., and K.J.M., performed electron microscopy on

microparticles. A.C.A. designed and performed in vitro transport experiments and imaged time-lapse microparticle release. A.C.A., X.X., Y.Z., W.T., A.M.B., E.R., A.R.D., J.L.S., J.Z., J.C., X.Lu, T.G., S.A., T.D.N., X.Le, and A.S.G., performed in vitro release experiments. A.C.A., X.X., S.B., Y.Z., W.T., E.R., and J.Z., performed in vitro stability experiments. W.T., S.B.W., and K.J.M. designed in vivo mouse experiments. W.T., K.J.M, J.L.S., S.Y.T., and S.R., performed in vivo experiments. A.C.A., C.B.S., J.D.O., and A.J. designed process development approaches. J.D.O. synthesized scaled-batches. S.B., D.M., and M.B.Z. designed the human clinical experiments. S.B. performed the human clinical experiments. A.C.A., L.E.F., R.L., S.B., and A.J., analyzed the data and wrote the manuscript. **Competing interests:** A.J., R.L, X.X., B.N., P.A.W., and L.W. are inventors on patent #9,649,279 held/submitted by the Massachusetts Institute of Technology and Tokitae LLC that covers micronutrient fortified salts that are thermally stable and release micronutrient payloads in the gastrointestinal tract. A.C.A., A.J., R.L., W.T. and X.X. are inventors on patent application #16/239284 submitted by the Massachusetts Institute of Technology that covers spray drying micronutrient microparticle formulations. **Data and materials availability:** All data associated with this study are present in the paper or supplementary materials.

Figures

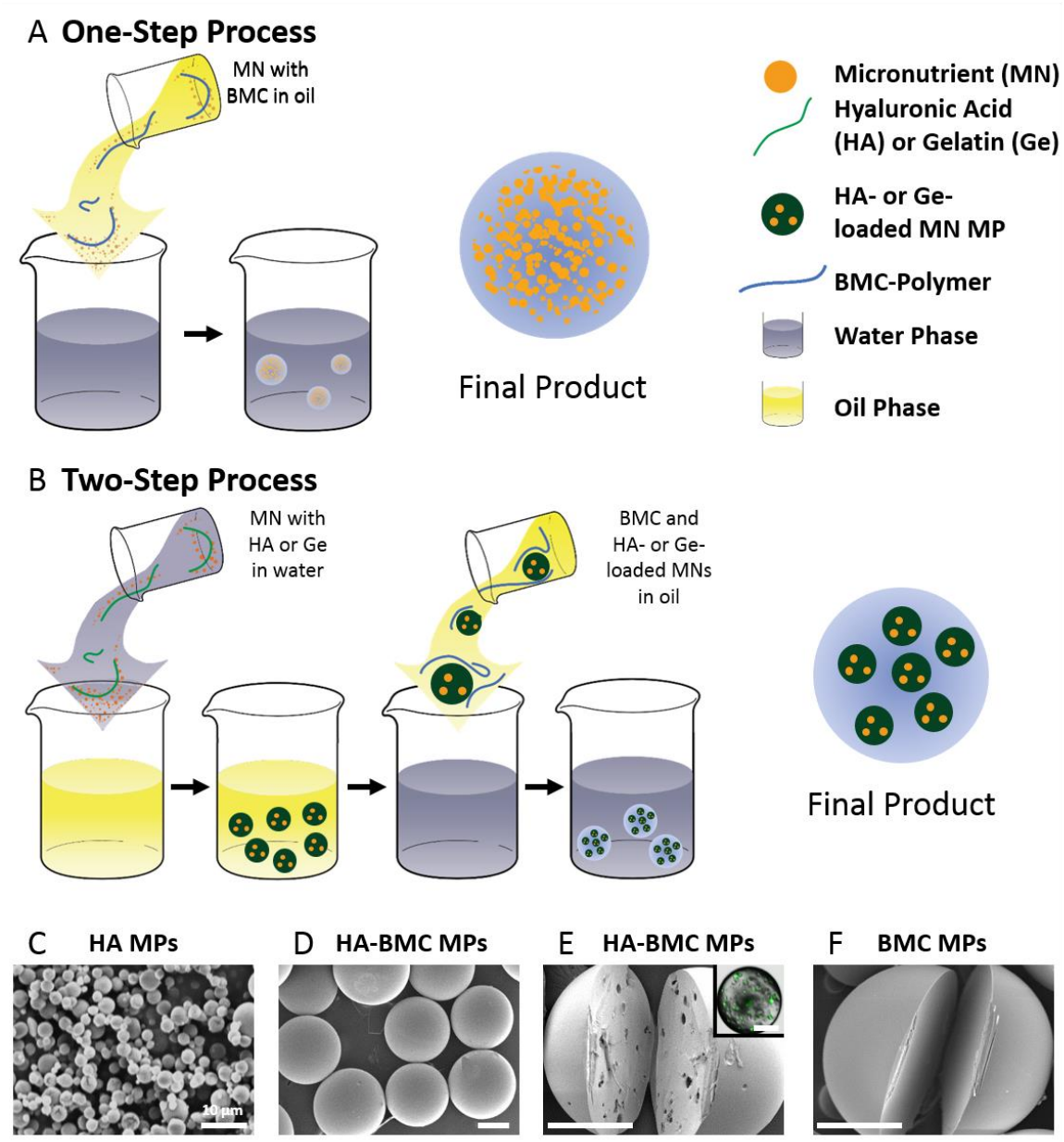

Fig. 1. Particle synthesis and characterization. Schematic representations of the (**A**) one-step and (**B**) two-step processes for formulating MPs. SEM images of (**C**) HA MPs, (**D**) HA-BMC MPs, (**E**) the cross section of an HA-BMC MP (inset: confocal image of an HA-BMC MP with fluorescently labeled HA), and (**F**) the cross section of a BMC MP. Scale bars = 100 μm unless otherwise noted. MP: microparticle

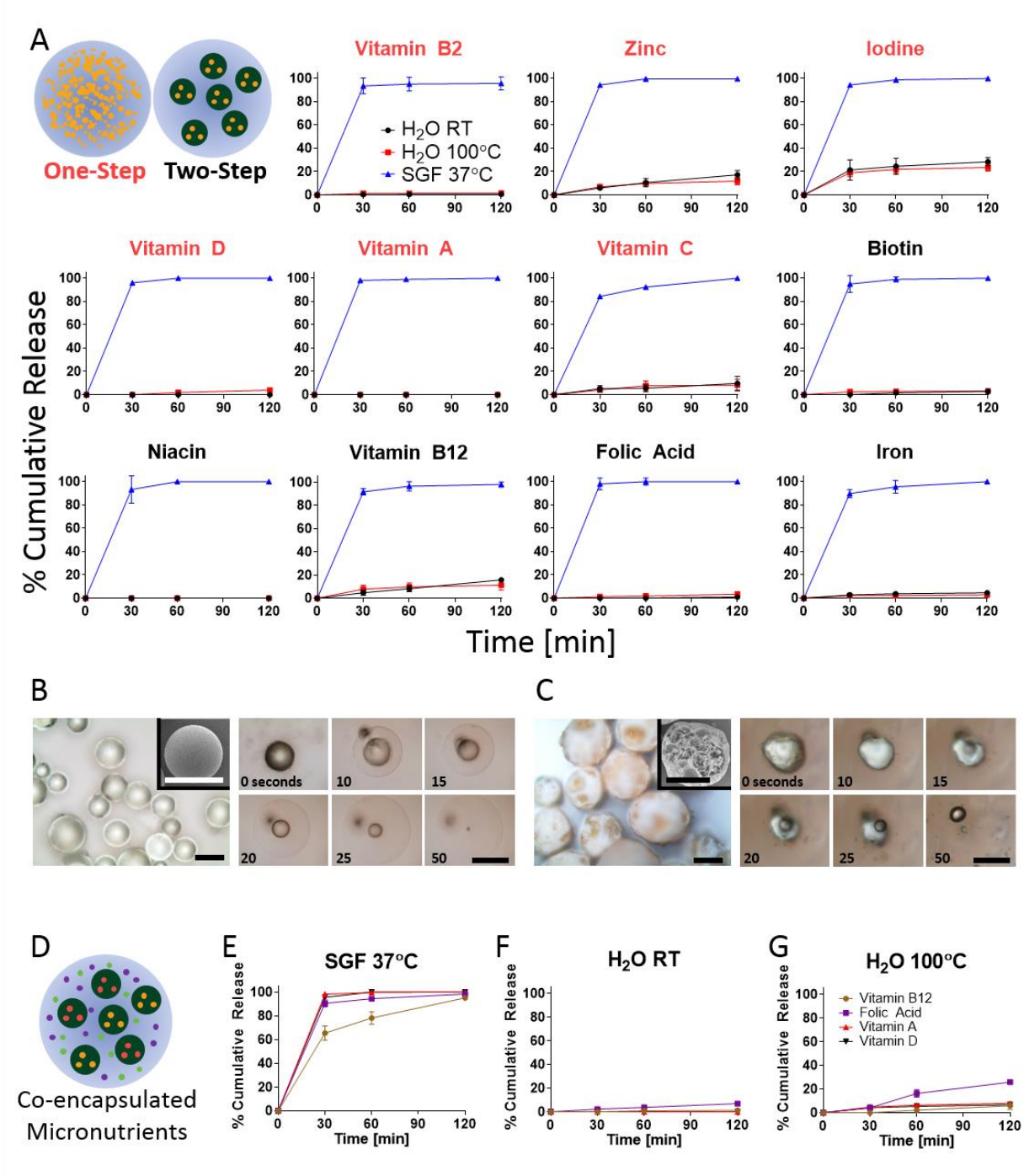

Fig. 2. Controlled release of micronutrients. (**A**) Percent cumulative release of 11 different individually encapsulated micronutrients in 37°C SGF, pH 1.5 (blue lines), and RT water (black lines) or boiling water (red lines). Schematic shows micronutrients encapsulated via one-step process (red text) versus two-step process (black text). (**B, C**) Representative bright-field images

and time-lapse release of (**B**) Vitamin A from BMC MPs and (**C**) iron from HA-BMC MPs in SGF (insets: SEMs). (**D**) Schematic of 4 co-encapsulated micronutrients [folic acid (purple), B12 (brown), vitamin A (red), and vitamin D (black)], percent cumulative release in (**E**) 37°C SGF, (**F**) RT water, and (**G**) boiling water. Error bars represent SD of the mean (n = 3). Scale bars = 200 μm. SGF: simulated gastric fluid; RT: room temperature

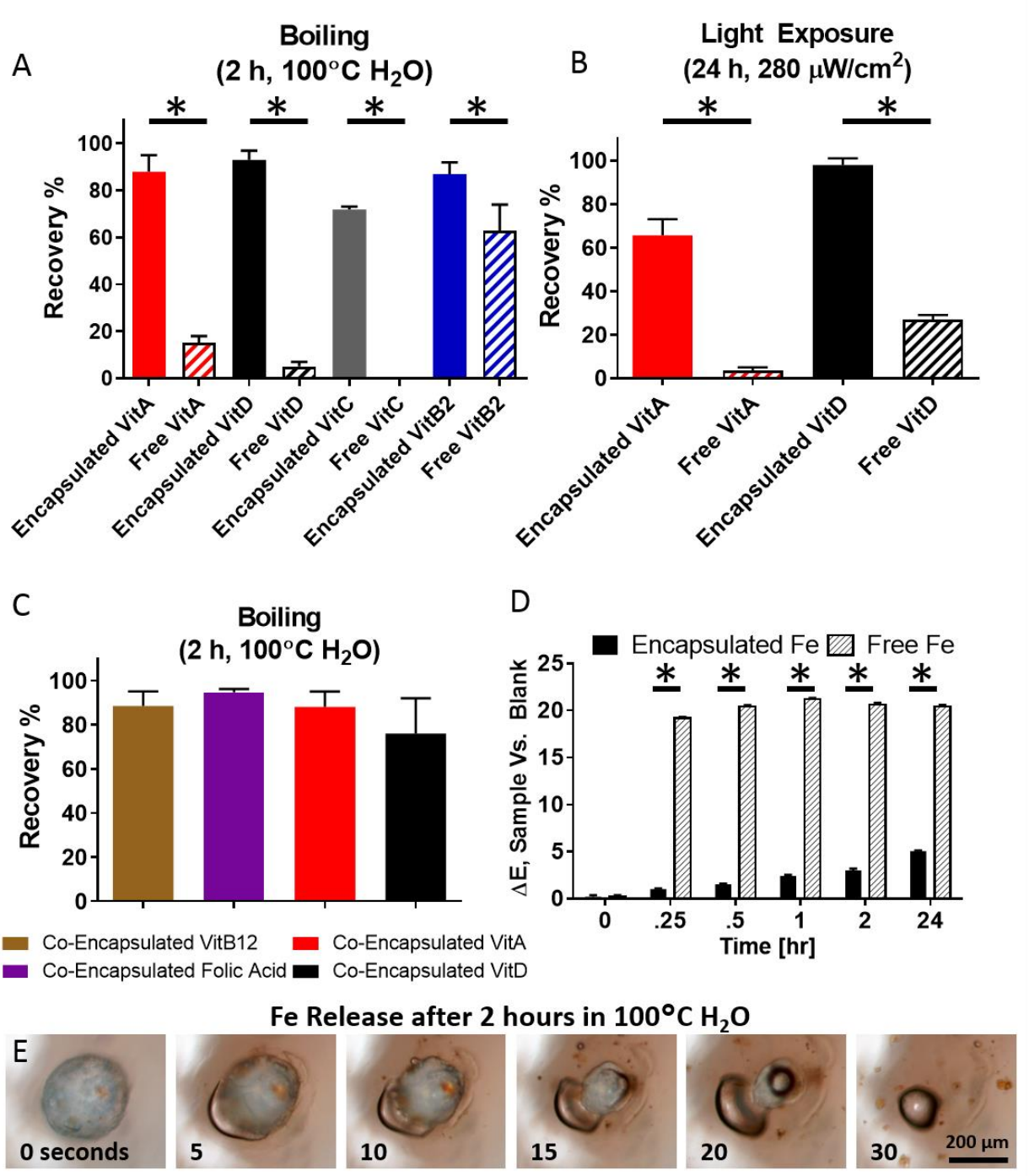

Fig. 3. Protection from heat, light, and chemical interactions. Recovery of individually encapsulated versus unencapsulated (free) micronutrients after exposure to (**A**) boiling water and (**B**) light. (**C**) Recovery of co-encapsulated micronutrients after boiling in water. (**D**) Time history of color change (ΔE), an indication of a chemical reaction between iron and polyphenols present

in banana milk, of lab-scale Fe-HA-BMC MPs versus unencapsulated (free) iron. (**E**) Time-lapse release of iron from HA-BMC MPs after boiling in water for 2 h room temperature and upon immersion in room temperature SGF. Error bars represent SD of the mean (n = 3). *$P < 0.05$ as determined by student t-test.

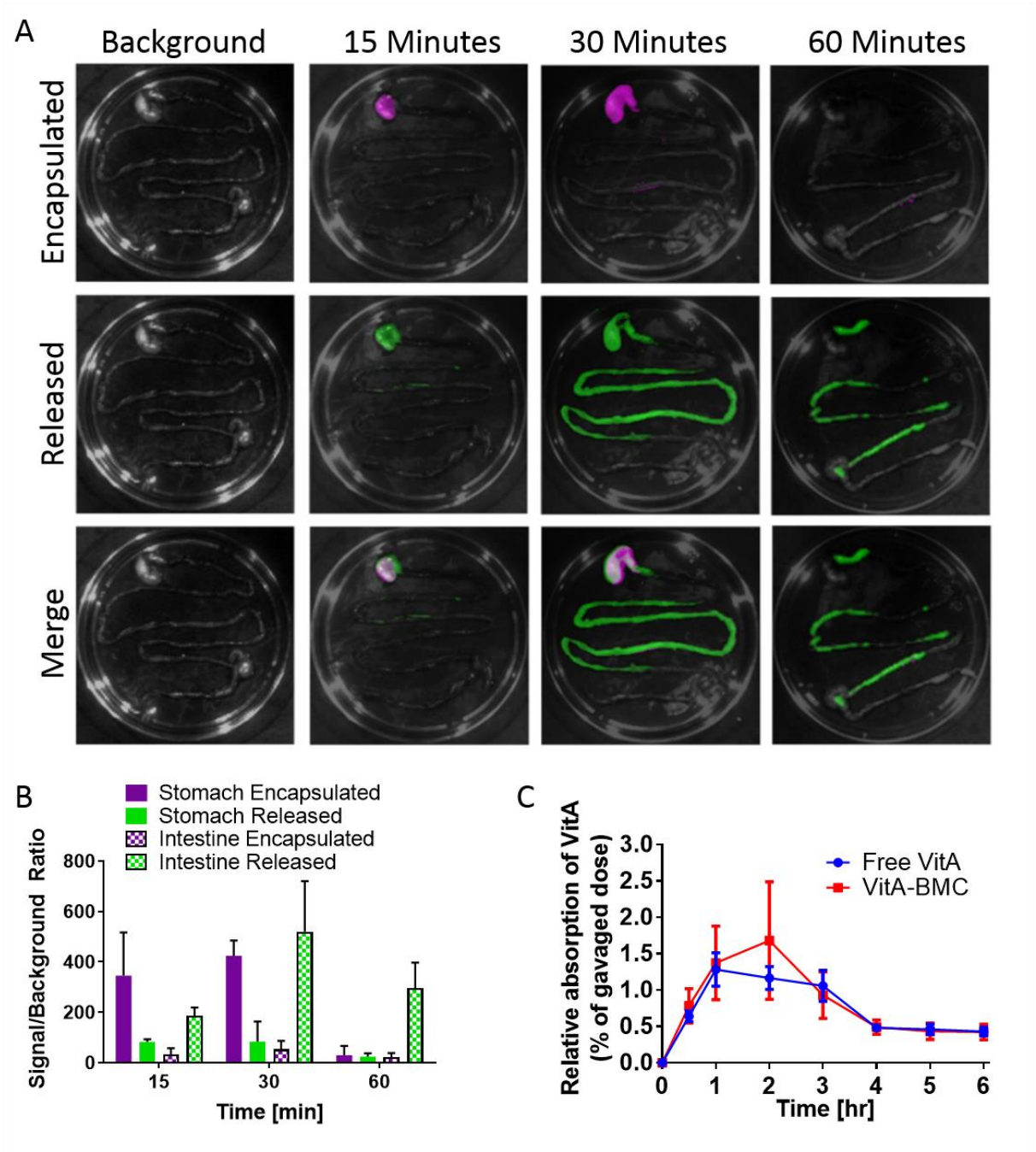

Fig. 4. In vivo release of a model dye and absorption of vitamin A. (**A**) Representative IVIS images (logarithmic scale) of explanted murine gastrointestinal tract harvested after oral administration of dye-loaded BMC MPs showing encapsulated dye (purple) and released dye (green) over 60 minutes. (**B**) Quantitative analysis of encapsulated dye in the stomach (solid purple bars), released dye in the stomach (solid green bars), encapsulated dye in the intestines (hatched

purple bars), and released dye in the intestines (hatched green bars). Error bars represent SD of the mean (n = 3). (**C**) Blood content of radiolabeled vitamin A over a 6 hour period after oral gavage of free vitamin A (blue lines) or VitA-BMC MPs (red lines). Error bars represent SEM (n = 6).

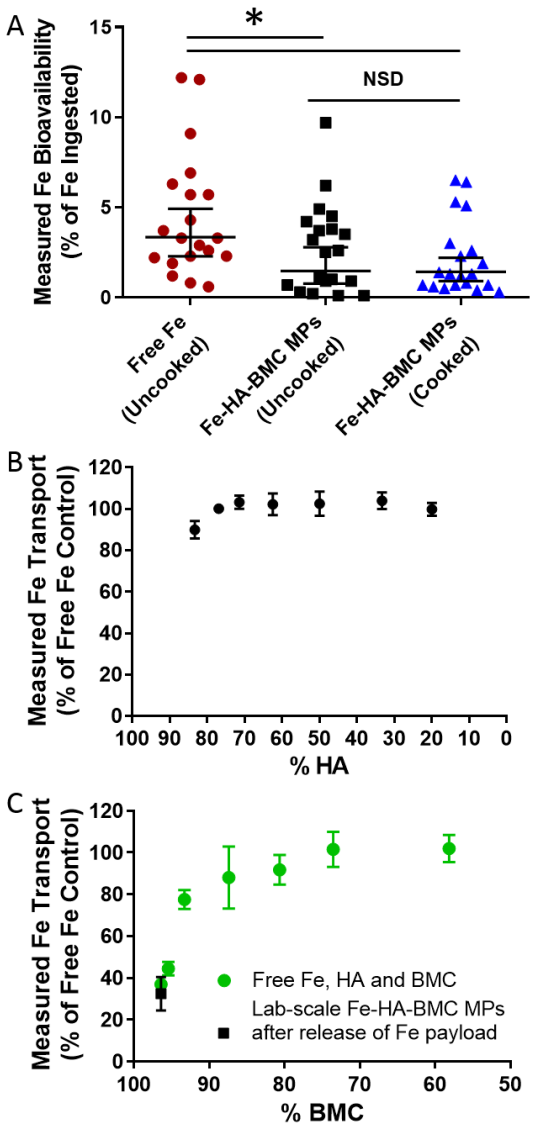

Fig. 5. Bioavailability of iron in humans and iron transport in an in vitro intestinal barrier model. (**A**) Iron bioavailability as assessed by erythrocyte iron incorporation in young women (n=20) after ingestion of unencapsulated (free) uncooked iron as $FeSO_4$ (red circles), encapsulated uncooked iron (black squares), and encapsulated cooked iron (blue triangles) and expressed as a percentage of the total amount that was ingested. Iron transported across a human in vitro intestinal barrier model after addition of iron in the presence of varying amounts of MP constituents (**B**) HA and (**C**) BMC and expressed as a percentage of transported free iron. Error bars in (**A**) represent

geometric means (n = 20) with 95% CI. *P < 0.05, free Fe and each encapsulated group as determined by post-hoc paired student t-test with Bonferroni correction. Error bars in (**B**, **C**) represent SD of the mean (n = 3). NSD: no significant difference

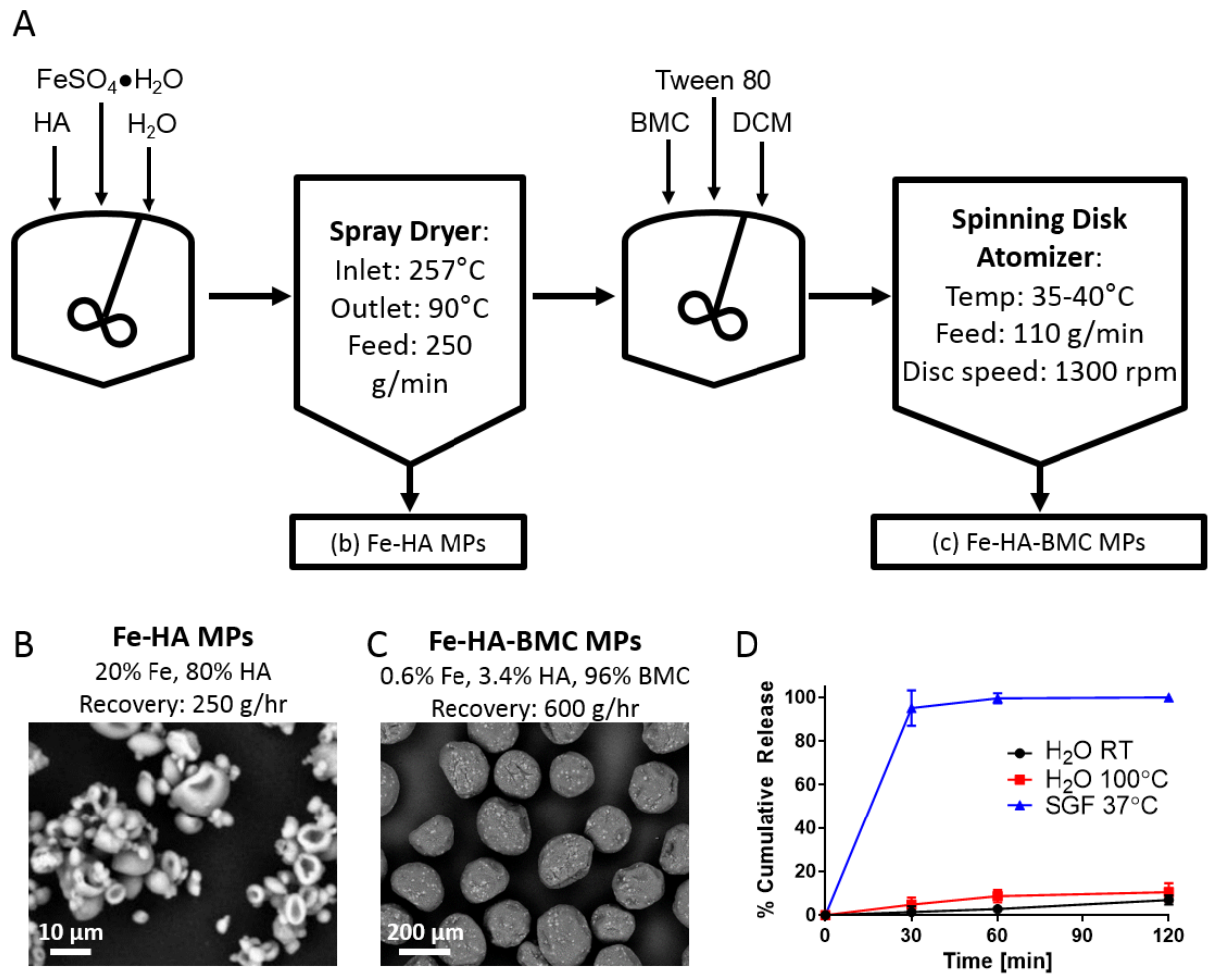

Fig. 6. Process development and scale-up. (**A**) Schematic showing the process for the scaled synthesis of 1 kg of Fe-HA-BMC MPs. SEM images of (**B**) the Fe-HA MP intermediate product and (**C**) the Fe-HA-BMC final product. (**D**) Iron release from scaled Fe-HA-BMC MPs in 37°C SGF, pH 1.5 (blue line), room temperature water (black line), and boiling water (red line). Error bars represent SD of the mean (n = 3).

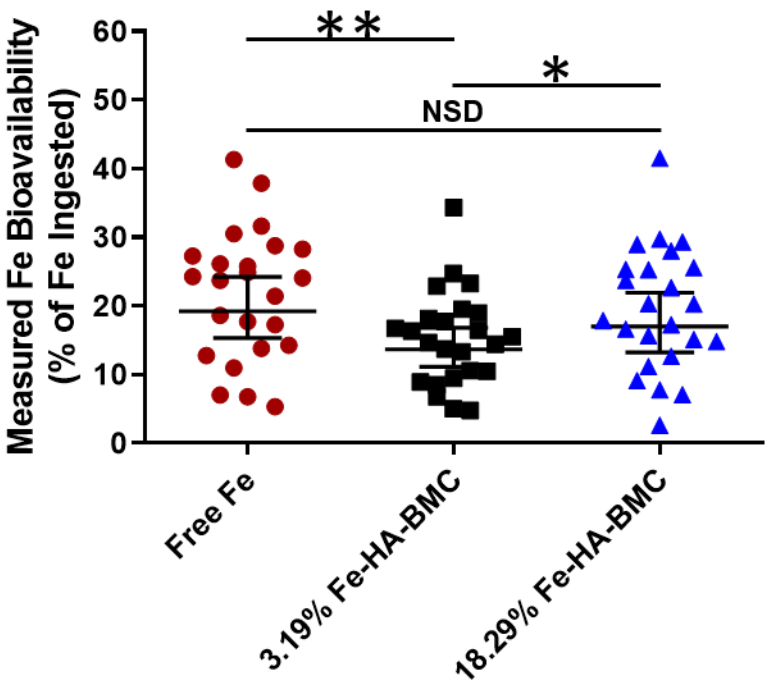

Fig. 7. Bioavailability of iron in humans from higher-loaded Fe-HA-BMC MPs. Iron bioavailability as assessed by erythrocyte iron incorporation in young women (n=24) after ingestion of free iron as $FeSO_4$ (red circles), 3.19% Fe-HA-BMC MPs (black squares), and 18.29% Fe-HA-BMC MPs (blue triangles) and expressed as a percentage of the total amount of iron that was ingested. Error bars represent geometric means (n = 24) and 95% CI. *$P < 0.05$, **$P < 0.01$ Significant effect of meal on iron absorption determined by linear mixed models, participants as random intercept, meal as repeated fixed factor, and post-hoc paired comparisons with Bonferroni correction $P < 0.05$. NSD: no significant difference

Supplementary Materials

Title: A heat-stable microparticle platform for oral micronutrient delivery

Authors: Aaron C. Anselmo[1,§,†], Xian Xu[1,§], Simone Buerkli[2,§], Yingying Zeng[1], Wen Tang[1], Kevin J. McHugh[1,#], Adam M. Behrens[1], Evan Rosenberg[1], Aranda R. Duan[1], James L. Sugarman[1], Jia Zhuang[1], Joe Collins[1], Xueguang Lu[1], Tyler Graf[1], Stephany Y. Tzeng[1], Sviatlana Rose[1], Sarah Acolatse[1], Thanh D. Nguyen[1,‡], Xiao Le[1], Ana Sofia Guerra[3], Lisa E. Freed[1,¥], Shelley B. Weinstock[4], Christopher B.Sears[5], Boris Nikolic[6], Lowell Wood[7], Philip A. Welkhoff[7], James D. Oxley[8], Diego Moretti[2,ǂ], Michael B. Zimmermann[2], Robert Langer[1*], and Ana Jaklenec[1*]

[§]These authors contributed equally to this manuscript.

Affiliations:

1. David H. Koch Institute for Integrative Cancer Research, Massachusetts Institute of Technology, Cambridge, MA 02139, USA
2. Institute of Food Nutrition and Health, ETH Zurich, 8092, Switzerland
3. Department of Chemistry & Chemical Biology, Harvard University, Cambridge, MA 02138, USA
4. Institute of Human Nutrition, Columbia University College of Physicians and Surgeons, NY, 10032 USA
5. Independent Scholar, Belmont, MA 02478, USA
6. Biomatics Capital, 1107 1st Avenue, Apartment 1305, Seattle, WA 98101, USA.
7. Institute for Disease Modeling, Bellevue, WA 98005, USA.
8. Southwest Research Institute, San Antonio, TX 78238 USA

† Present address: Division of Pharmacoengineering and Molecular Pharmaceutics, Eshelman School of Pharmacy, University of North Carolina at Chapel Hill, Chapel Hill, NC, 27599, USA.

Present address: Department of Bioengineering, Rice University, Houston, TX, 77030

‡ Present address: Department of Mechanical Engineering, University of Connecticut, Storrs, CT 06269, USA.

¥ Present address: Media Lab, Massachusetts Institute of Technology, Cambridge, Massachusetts, 02139, USA

ǂ Present address: Nutrition Group, Health Department, Swiss Distance University of Applied Sciences, Regensdorf, CH-8105, Switzerland

[*] Corresponding author. Email: jaklenec@mit.edu (A.J.); rlanger@mit.edu (R.L.);

List of Supplementary Materials

Materials and Methods

Materials

All materials were from Sigma unless otherwise specified. The BMC polymer, poly(butylmethacrylate-co-(2-dimethylaminoethyl)methacrylate-co-methylmethacrylate) (1:2:1), was from Evonik Industries, where Eudragit E PO-powder and Eudraguard Protect-powder were respectively used to formulate small scale and larger scale batches of MPs. The HA was from Lifecore Biomedical. The Ge was from Sigma; The Iron (ferrous sulfate, $FeSO_4 \cdot 7\ H_2O$) was from Sigma; Iodine (potassium iodate, KIO_3) was from Sigma; Zinc (zinc sulfate, $ZnSO_4$) was from Sigma. The Vitamin A (retinyl palmitate) was from Alfa Aesar; Vitamin B2 (riboflavin) was from Sigma; Niacin (nicotinic acid) was from Sigma; Vitamin B7 (biotin) was from Sigma; Vitamin B9 (folic acid) was from Sigma; Vitamin B12 (cobalamin) was from Sigma; Vitamin C (ascorbic acid) was from Sigma; Vitamin D3 (cholecalciferol) was from Sigma. The dichloromethane was from Sigma. The SGF was from Ricca Chemical Company.

Formulation of HA MPs

HA MPs were formulated using a modified inverse emulsion technique (*65*). Blank HA MPs were prepared by homogenizing an HA solution (Low molecular weight HA, Mn = 384 kDa, Mw = 803 kDa; 1 wt % in de-ionized water) in mineral oil (30 ml) containing 120 µl of Span80 for 10 min using a Silverson L5M-A laboratory mixer (Silverson Machines, Inc.). To prepare the lab-scale MN encapsulated HA MPs, vitamins folic acid, B12 and/or ferrous sulfate heptahydrate were dissolved in the HA aqueous solution (1 wt% in 2 ml of de-ionized water) as described in **table S2**. The resulting solution was then used for the preparation of the emulsion as described above. The aqueous phase of the emulsion was allowed to evaporate for 24 hours at 45°C with constant stirring. The obtained HA MPs were then isolated by centrifugation at 3000 rpm for 5 min and thoroughly washed by hexane and acetone before drying under vacuum overnight. To prepare fluorescently labeled HA MPs, HA derivatives containing aldehyde groups (HA-CHO) were first synthesized using sodium periodate following reported procedures (*66*). Since oxidation causes

chain cleavage of the HA (*66*), high molecular weight HA (Mn=1096 KDa, Mw=2698 KDa) was used in this case. The molecular weight of obtained HA-CHO was analyzed by gel permeation chromatography (GPC). The degree of modification was quantified as 65% by an iodometry method following reported methods (*67*). To formulate fluorescent HA MPs, HA-CHO and unmodified HA were mixed with a weight ratio of (1:1) and were then used to prepare the MPs by the inverse emulsion method as described above. For dye labelling, one milligram of the HA-MP containing aldehyde groups was dispersed in a methanol solution of CF405M (fluorescent dye containing aminooxy group, Biotium Inc.). Acetic acid (5 µl) was added to accelerate the reaction. The reaction was then allowed to proceed for 12 hours at room temperature. The dye labelled particles were collected by centrifugation (3000 rpm, 5min), and thoroughly washed using methanol before drying under vacuum.

Morphological MP characterization

Three different microscopic methods were used to characterize the MP size, morphology, and cross sections; namely, optical microscopy (Olympus MX40), scanning electron microscopy (JEOL 5910 SEM), and confocal microscopy (Zeiss LSM 700 Laser Scanning Confocal). Dry MPs were coated with Pt/Pd before SEM imaging. Dye labeled HA MPs were visualized by the confocal microscope at an excitation wavelength at 405 nm, with a band pass filter of 420-475 nm. Reported mean particle diameters were estimated using ImageJ based on at least 20 counts of the particles from SEM images.

Clinical study: Iron absorption studies, procedure, and laboratory analyses

Study procedure: Study 1 was conducted in March – April in 2016 at the Laboratory for Human Nutrition (HNL) in Zürich. 118 participants attended the screening 1-2 weeks before test meal administration, weight and height were measured, a blood sample for Hb, PF and CRP measurement was collected, and 20 participants meeting the inclusion and exclusion criteria were invited to participate. Test meals A, B and C were administered on 3 consecutive days (study days D1, 2 and 3), the subjects were instructed to consume no solid food after 20.00 h and no fluids after 24.00 h the evening before test meal administrations. They consumed the test meals between 07.00-09.00 h each morning under direct supervision. After consuming the entire maize porridge test meal, the bowl was rinsed twice with 10 ml water and participants drank the rinsing liquid and remained fasting (no food nor drink) for 3 hours after test meal administration. On D17, a venous blood sample was taken for determination of Hb, PF, CRP, and determination of stable iron isotope ratio into the erythrocytes. The test meal consisted of porridge made from 50 g whole maize flour, served with 30 g vegetable sauce (44% cabbage, 21% carrots, 21% zucchini, 12% onions, 2% oil) and 1 g salt. The amount of iron added to the porridge through fortified salt would correspond to a level of 80 ppm iron in directly fortified maize flour. The maize flour contained 1.52 mg Fe/100 g and 736.8 mg phytic acid /100 g. Each test meal contained 50 mg of maize and an additional 4 mg of fortification iron; thus, total iron and phytic acid content in the test meals was 4.8 mg Fe and 368 mg phytic acid, resulting in an iron to phytic acid ratio of 1:6.5. Ascorbic acid content of the test meals was negligible, 0.4 mg/meal. Thus, the test meal matrix was an inhibitory matrix in terms of iron absorption (*45*). Nanopure water (300 ml) was served as a drink with the test meals. The vegetable sauce was prepared in bulk and stored frozen in portions until administration. Maize flour was precooked as follows: on the night before test meal administration, each individual maize portion was mixed with warm 18 MΩ/cm water, preheated in the microwave (1 min, 600 W), and then baked in an oven at 100° C for 60 min. After overnight refrigeration, on the administration

day, maize porridge was preheated in the microwave for 1 minute at 600 W, and then cooked for further 30 min in the oven (100°C). The test meals with the cooked iron-loaded BMC-HA MPs were fortified before the microwaving step. The test meals with the non-cooked iron-loaded BMC-HA MPs were cooled down for 10 minutes to just under 50°C before the microspheres were added. The defrosted and preheated vegetable sauce was added just before serving.

Study 2 was conducted between April – July 2018 at the HNL. Prior the test meals, 77 participants attended screening, weight and height were measured, a blood sample for Hb, PF and CRP measurement was collected, 24 eligible participants were invited to participate. The participants were instructed with the same fasting conditions as in study 1. After consuming the entire bread test meal, the participants were instructed to consume all bread crumbs that had fallen into the plate. As in study 1 the participants remained fasting for 3 hours after test meal administration. The 9 test meals were administered in 3 blocks, within the first week, 3 test meals were administered on 3 consecutive days (D1, 2, and 3). On D22 a blood sample was drawn for determination of Hb, PF, CRP, and determination of stable iron isotope ratio into the erythrocytes. The next block of test meals was administered on D22, 23 and 24, and again on D43 a blood sample was drawn, within that week the last block of test meals was administered on D43, 44 and 45. The last blood sample was taken on D64. All bread roll test meals were prepared the afternoon before test meal administration, two doughs were prepared made of 1 kg refined wheat flour each, 5.5 g salt, 14 g dry yeast and 650 g of nanopure water, the dough was kneaded for 10 min using a kitchen machine. And then weighed into portions of 100 g. 1/3rd of the portion was fortified with the microspheres, and 2/3rd of the portion was used to cover the fortified core. The amount of iron added to the bread was 67 ppm iron in wheat flour. After forming, the bread rolls were fermented for 45 minutes at 30°C and 80% relative humidity, and then baked for 20 minutes at 190°C. They cooled down on a cooling rack and wrapped in paper and stored at RT until consumption the next morning. The bread rolls consisted of 59.9 g wheat flour, 0.3 g of salt and 0.8 g of dry yeast, with the bread roll 300 ml of nanopure water was served as a drink.

Test meal analysis: Sample analyses of the test meals were done in triplicate. Iron concentrations of the maize flour and bread rolls were measured by graphite-furnace atomic absorption spectrophotometry (AA240Z; Varian) after mineralization by microwave digestion (MLS ETHOSplus, MLS). The phytate concentration of the maize flour and the bread roll was measured by spectrophotometry Makower method, in which iron was replaced by cerium in the precipitation step (*68*). Ascorbic acid concentration in the vegetable sauce was measured by HPLC (Acquity H-Class UPLC System; Waters AG) after stabilization in 10 % metaphosphoric acid.

Blood analysis: Hb was measured by using a Coulter Counter (Study 1: Beckman Coulter, CA, USA; Study 2: Sysmex XN-350). PF and CRP was measured by using immunoassays (Study 1: Siemens Healthcare IMMULITE 2000; study 2: IMMULITE1000). Anemia was defined as Hb < 12 g/dL, Iron deficiency (ID) as PF < 15 mg/L and ID anemia as Hb < 12 g/dL and PF < 15 mg/L (*69*). Whole blood samples collected on D17 (study 1), and in study 2 on D22, 43, and 64 were mineralized by using HNO_3 and microwave digestion followed by separation of the iron from the blood matrix by anion-exchange chromatography and a precipitation step with ammonium hydroxide (*70*). All isotopic analyses were performed by using MC-ICP-MS (Neptune; Thermo Finnigan). The amounts of ^{57}Fe, ^{54}Fe and ^{58}Fe isotopic labels in blood 14 d after administration of the test meals were calculated on the basis of the shift in iron isotope ratios and on the estimated amount of iron circulating in the body. Circulating iron in the body was calculated based on hemoglobin and blood volume, derived from the participant's height and weight (*71*). Fractional absorption (FIA) was calculated based on the assumption of an 80% incorporation of absorbed

iron into the red blood cells. In study 2, the isotopic ratio value of D22 and 43 served as a new baseline value for the after test meal administrations. Relative bioavailability (RBV) of iron was calculated as follows: $100/FIA_{\text{reference meal}}*FIA_{\text{test meal}}$.

Supplemental Figures

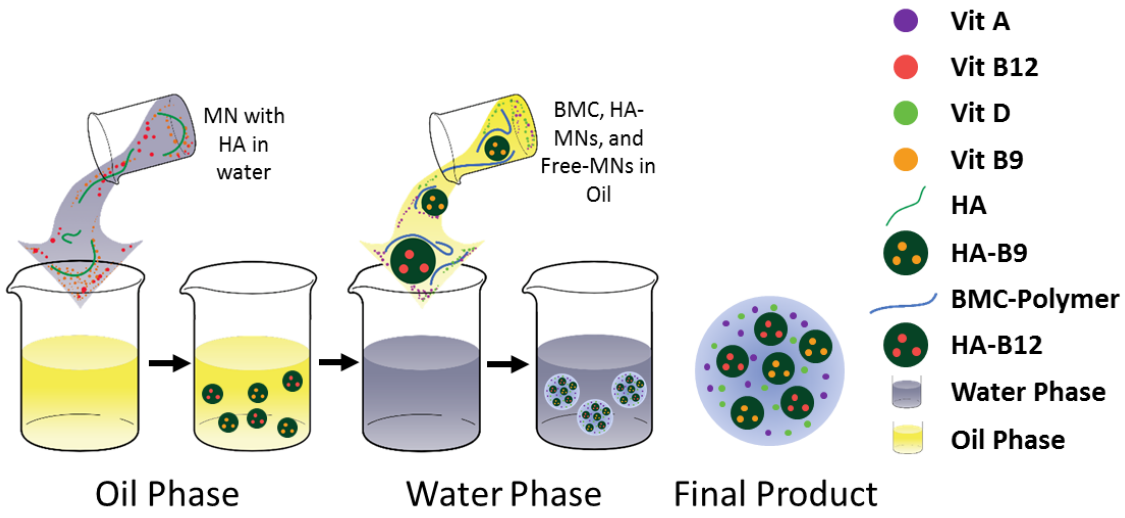

Fig. S1. Lab-scale co-encapsulation of micronutrients. Schematic representations of the two-step process for formulating co-encapsulated micronutrient MPs.

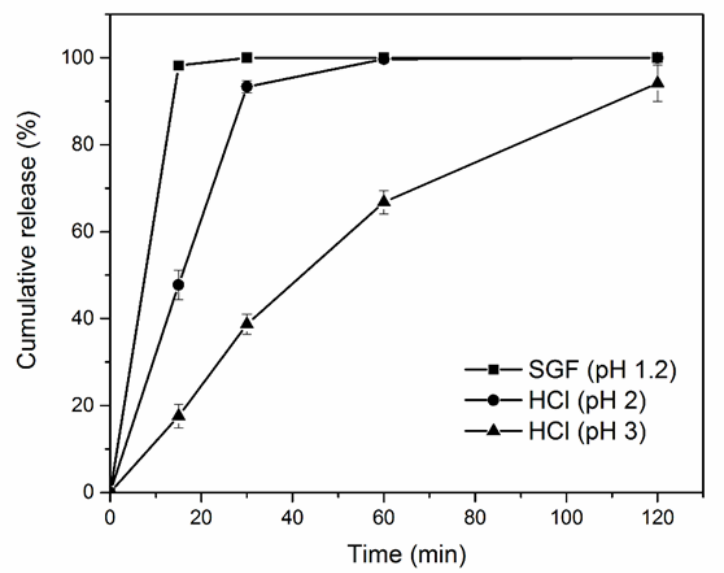

Fig. S2. Vitamin B12 release as a function of pH. Release of vitamin B12 from HA-BMC MPs in SGF (black squares), pH 2 HCl (black circles), and pH 3 HCl (black triangles). Error bars represent SD of the mean (n = 3).

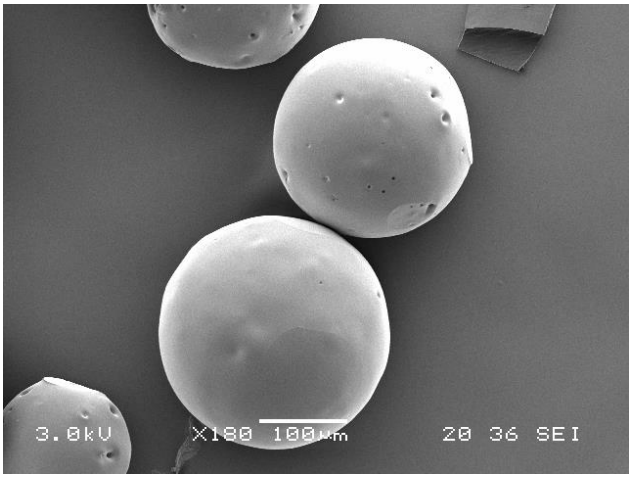

Fig. S3. HA-BMC MP electron micrograph after 2 hours in boiling water. SEM image of HA-BMC MPs after exposure to boiling water for 2 hours.

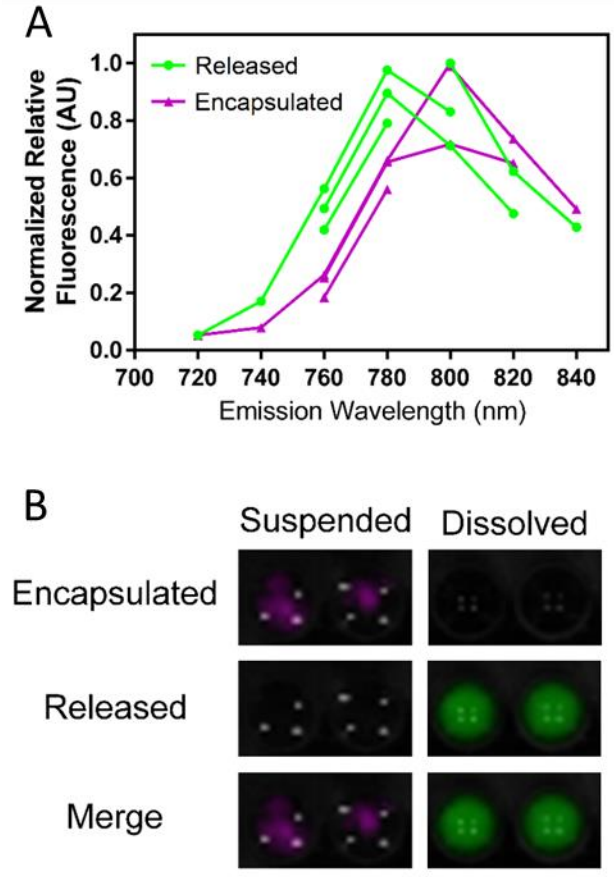

Fig. S4. Spectral fingerprinting of DiR-loaded MPs. (**A**) Spectral fingerprint and (**B**) representative IVIS images of a DiR-loaded BMC MPs when encapsulated (purple) or released in SGF (green).

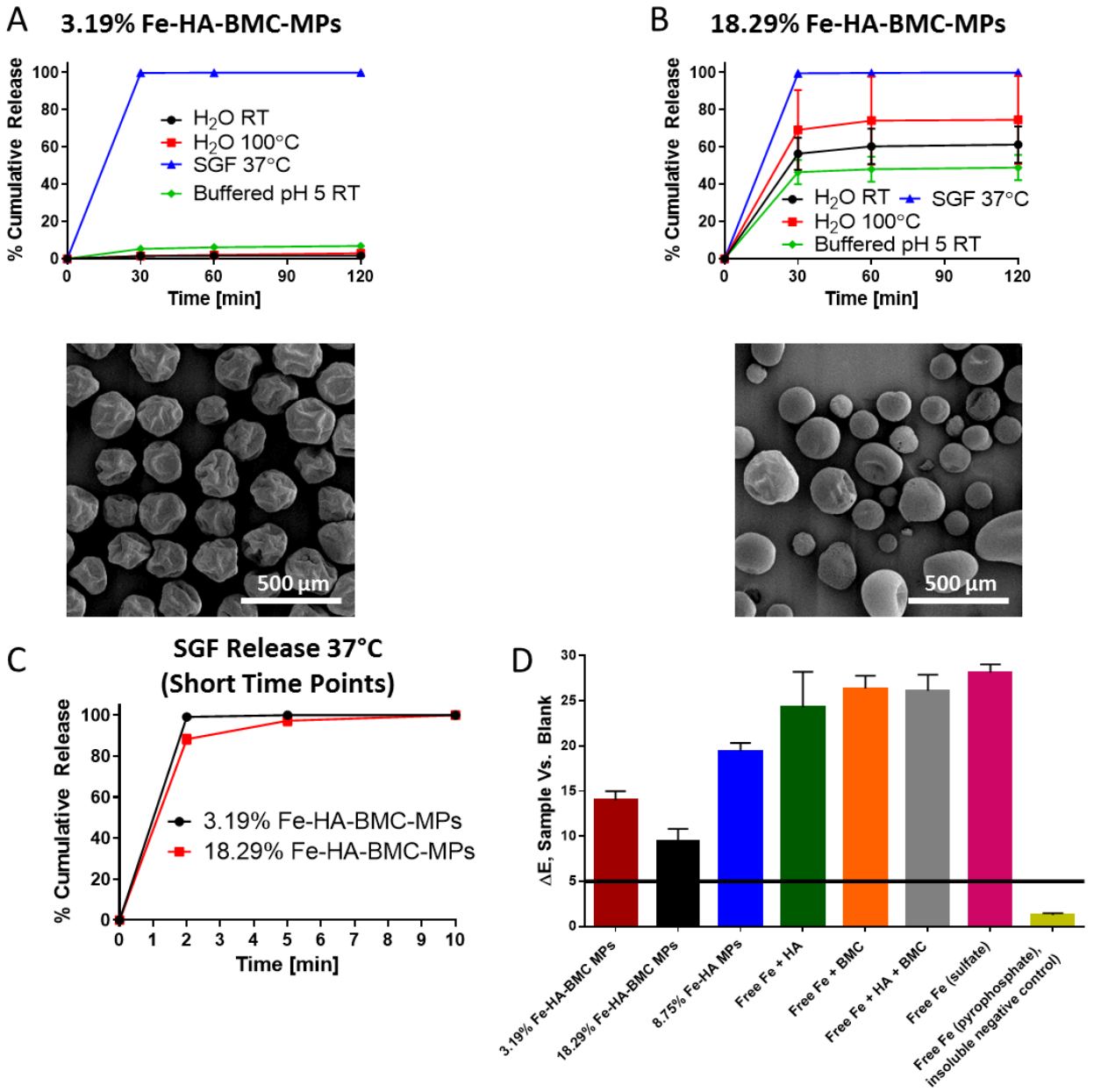

Fig. S5. Release, electron micrographs, and time history of color change for 3.19% and 18.29% Fe-HA-BMC MPs. (**A**) Release of iron from, and SEM image of, 3.19% Fe-HA-BMC MPs. (**B**) Release of iron from, and SEM image of, 18.29% Fe-HA-BMC MPs. (**C**) Release of iron from 3.19% and 18.29% Fe-HA-BMC MPs at short time points in SGF. (**D**) Sensory performance of scaled Fe-HA-BMC MPs and their individual constituents in a food matrix (banana milk), compared to $FeSO_4$ and FePP, at 60 ppm Fe. Absolute color change ΔE±SD is given at 120 min against the non-fortified matrix. Horizontal line represents the threshold below which ΔE cannot be detected. Error bars represent SD of the mean (n = 3).

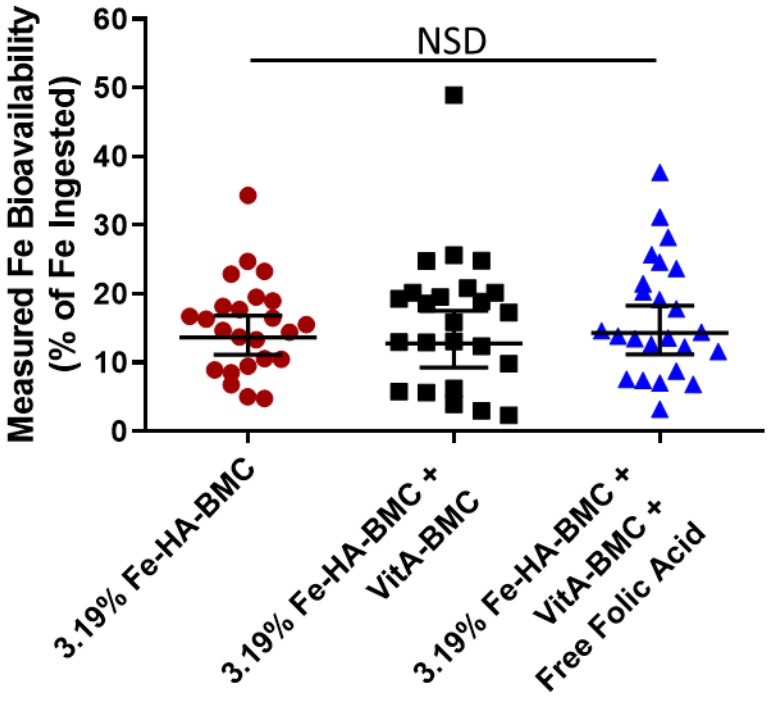

Fig. S6. Evaluation of iron absorption from 3.19% Fe-HA-BMC MPs in humans when co-administered with VitA-BMC MPs and free folic acid. Iron bioavailability as assessed by erythrocyte iron incorporation in young women (n=24) after ingestion of 3.19% Fe-HA-BMC MPs (red circles), 3.19% Fe-HA-BMC MPs with VitA-BMC MPs (black squares), and 3.19% Fe-HA-BMC MPs with VitA-BMC MPs and free folic acid. These values are expressed as a percentage of the total amount of iron that was ingested. Error bars represent geometric means (n = 24) and 95% CI. Significant effect of meal on iron absorption determined by linear mixed models, participants as random intercept, meal as repeated fixed factor, and post-hoc paired comparisons with Bonferroni correction $P < 0.05$. NSD: no significant difference

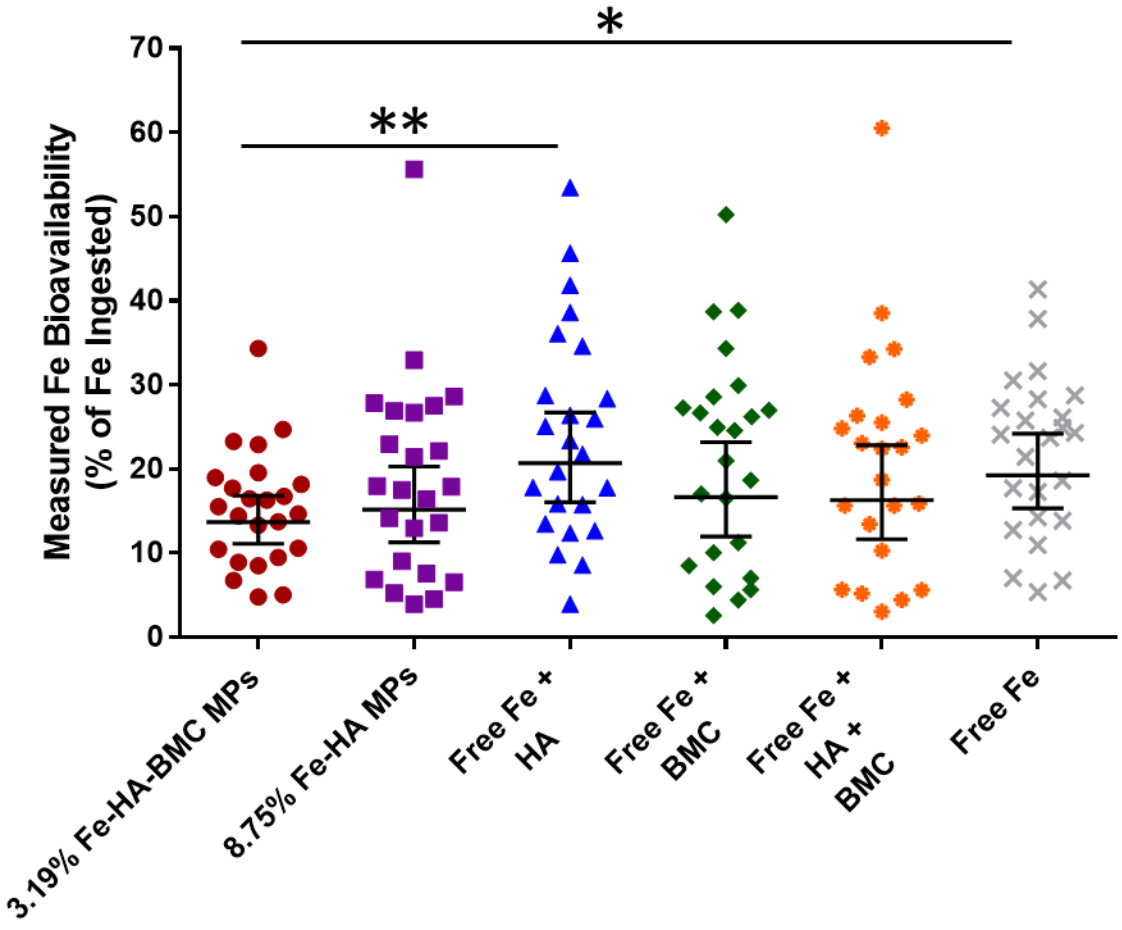

Fig. S7. Comparison of iron absorption from 3.19% Fe-HA-BMC MPs with each MP constituent both individually and in combination. Iron bioavailability as assessed by erythrocyte iron incorporation in young women (n=24) after ingestion of 3.19% Fe-HA-BMC MPs (red circles), 8.75% Fe-HA MPs, free iron with free HA (purple squares), free iron with free BMC (green diamonds), free iron with free HA and free BMC (orange stars), free iron (grey crossbars). These values are expressed as a percentage of the total amount of iron that was ingested. Error bars represent geometric means (n = 24) and 95% CI. *P < 0.05, **P < 0.01 Significant effect of meal on iron absorption determined by linear mixed models, participants as random intercept, meal as repeated fixed factor, and post-hoc paired comparisons with Bonferroni correction P < 0.05. NSD: no significant difference

Supplemental Tables

Table S1. Polymers evaluated as potential MP matrix materials. Polymers were evaluated based on the need to address key issues limiting current food fortification technologies, specifically enabling: (i) the encapsulation of both water-soluble and fat-soluble micronutrients, (ii) rapid release in the stomach to ensure intestinal absorption, and (iii) the protection of the encapsulated micronutrients from high temperature, moisture, and oxidizing chemicals during cooking or storage. To assess whether polymers could address these challenges, we selected specific requirements for the chosen polymer. Requirement 1 (Column 2) is that the polymer must be soluble in organic solvents to facilitate formulation with fat-soluble micronutrients. Requirement 2 (Column 3) is that the polymer must be soluble in gastric conditions (below pH 5) to enable burst release in the stomach and subsequently intestinal absorption. Requirement 3 (Column 4) is that the polymer must currently be used in either pharmaceuticals or dietary supplements to enable clinical translation. Requirement 4 (Column 5) is that the polymer must be stable at high temperatures and high humidity to ensure that the encapsulated micronutrients will be protected during cooking and storage. Shaded boxes indicate requirements that have been met by the polymer. Only the pH-responsive basic methacrylate copolymer (BMC), Eudragit E PO, met the requirements for each column and as such was chosen to be the encapsulating matrix. Abbreviations: Methanol: MeOH; Ethanol: EtOH; Acetone: Ace; Dichloromethane: DCM; Isopropanol: IPA.

Polymer (Commercial Product)	**Solvent Solubility**	**Aqueous Solubility**	**GRAS Status/ History of Use**	**Storage Stable at High Temperatures and Humidity**	**Refs**
Requirements	*Solubility in organic solvents required to encapsulate fat-soluble micronutrients*	*pH <5 aqueous solubility required to enable stomach release*	*Use in pharmaceutical or dietary products required for safety and approval*	*Stability required to ensure that micronutrients remain viable after cooking or long-term storage*	
Polyvinyl Acetate Phthalate (Opadry 91 Series, Sureteric)	MeOH, EtOH, EtOH:Ace, MeOH:DCM, IPA:DCM, IPA:H_2O	Aqueous ≥pH 5	Listed in FDA inactive ingredients for approved drug products	Yes	(*72, 73*)
Cellulose Acetate Phthalate (Cellacefate, Eastman C-A-P)	Ace, Ace:EtOH, Ace:IPA, Ace:MeOH, Ace:DCM, DCM:EtOH	Aqueous ≥pH 6	Listed in FDA inactive ingredients for approved drug products	No: hydrolyze at high temperature and humidity	(*74-76*)
Hypromellose Phthalate	EtOH:DCM, EtOH:Ace, EtOH:H_2O	Aqueous ≥pH 5	Listed in FDA inactive ingredients for approved drug products	No: hydrolyze at high temperature and humidity	(*77, 78*)

Hypromellose Acetate Succinate (AQOAT, AquaSolve)	MeOH, Ace, EtOH:DCM, EtOH:H_2O	Aqueous ≥pH 5-6.5	Listed in FDA inactive ingredients for approved drug products	No: hydrolyze at high temperature and humidity	(*79, 80*)
Shellac	MeOH, EtOH, IPA	Aqueous >pH 7	Listed in FDA inactive ingredients for approved drug products	No: polymerize at high temperature and humidity	(*81-85*)
Chitosan	No	Aqueous <pH 6.5	Self-affirmed GRAS	No: hydroscopic and variations in molecular weight, deacetylation, and purity	(*86-88*)
Ethyl methacrylate-methacrylic acid copolymer (1:1 copolymer ratio) (Eudragit L 100-55)	MeOH, EtOH, IPA, Ace	Aqueous >pH 5.5	Listed in FDA inactive ingredients for approved drug products	Yes	(*50, 89, 90*)
Methyl methacrylate-methacrylic acid copolymer (1:1 copolymer ratio) (Eudragit L 100)	MeOH, EtOH, IPA, Ace	Aqueous >pH 6	Listed in FDA inactive ingredients for approved drug products	Yes	(*50, 89, 90*)
Methyl methacrylate-methacrylic acid copolymer (1:2 copolymer ratio) (Eudragit S 100)	MeOH, EtOH, IPA, Ace	Aqueous >pH 7	Listed in FDA inactive ingredients for approved drug products	Yes	(*50, 89, 90*)
Methyl methacrylate-dimethylaminoethyl methacrylate-butyl methacrylate copolymer (1:2:1 copolymer ratio) (Eudragit E PO, Eudraguard)	MeOH, EtOH, IPA, Ace, DCM, ethyl acetate	Aqueous <pH 5	Listed in FDA inactive ingredients for approved drug products	Yes	(*50, 91, 92*)

Table S2. Formulation parameters and loadings for lab-scale microparticles. All values are mean ± SD. MN = Micronutrient.

Lab-scale BMC microparticles										
MN	MN (mg)	BMC (mg)	Loading (µg/mg)	Loading %	Encapsulation Efficiency (EE) (%)					
Vitamin A	10	100	73 ± 7	7.3 ± 0.7	80 ± 8					
Vitamin B2	15	200	67 ± 2	6.7 ± 0.2	96 ± 3					
Vitamin C	20	200	63 ± 2	6.3 ± 0.2	69 ± 2					
Vitamin D	2	100	12 ± 1	1.2 ± 0.1	61 ± 5					
Zinc	17	100	11 ± 1	1.1 ± 0.1	7.6 ± 0.7					
Iodine	5	100	21 ± 3	2.1 ± 0.3	44 ± 6					
Lab-scale HA-BMC microparticles										
	HA-particle					BMC-HA microsphere				
MN	MN (mg)	HA (mg)	Loading (µg/mg)	Loading %	EE (%)	HA-MN (mg)	BMC (mg)	Loading (µg/mg)	Loading %	EE (%)
Fe	30	20	185 ± 5	18.5 ± 0.5	31 ± 2	11.3	200	6.0 ± 0.1	0.6 ± 0.01	61 ± 1
Vitamin B9	5	20	117 ± 21	11.7 ± 2.1	59 ± 11	5.2	100	1.7 ± 0.1	0.17 ± 0.01	29 ± 2
Vitamin B12	5	20	141 ± 17	14.1 ± 1.7	71 ± 9	2.5	100	2.3 ± 0.1	0.23 ± 0.01	67 ± 3
Lab-scale Ge-BMC microparticles										
	Ge-particle					BMC-Ge microsphere				
MN	MN (mg)	Ge (mg)	Loading (µg/mg)	Loading %	EE (%)	Ge-MN (mg)	BMC (mg)	Loading (µg/mg)	Loading %	EE (%)
Vitamin B3	15	20	58 ± 5	5.8 ± 0.5	14 ± 1	5	200	0.4 ± 0.1	0.04 ± 0.01	28 ± 7
Vitamin B7	17	20	320 ± 5	32 ± 0.5	70 ± 1	3	200	3.5 ± 0.6	0.35 ± 0.06	74 ± 13

Table S3. Subject characteristics of human study 1 and 2. All female, no significant difference in baseline characteristics between the study populations[a].

Baseline subject characteristics of study participants for human study 1 and 2		
Characteristics	Study 1	Study 2
n (number of subjects)	20	24
Age[b] [year]	22.8 ± 3.5	22.4 ± 1.9
Height [meter]	1.66 ± 0.06	1.64 ± 0.06
Weight [kg]	57.3 ± 4.1	57.8 ± 6.2
Body Mass Index [kg/m^2]	20.8 ± 1.5	21.3 ± 1.4
C-Reactive Protein[c] [mg/L]	0.62 (0.36, 1.07)	1.07 (0.72, 1.59)
Plasma Ferritin [µg/L]	11.6 (9.4, 14.5)	13.2 (10.5, 16.5)
% Iron Deficient[d] (PF < 15 µg/L)	65	58
Hemoglobin [g/L]	13.4 ± 0.85	13.2 ± 0.95
% Anemic[e] (Hemoglobin < 120 g/L)	5	8
% IDA[f]	5	4

[a]independent t-test, $P < 0.05$

[b]all such values are mean ± SD

[c]all such values are geometric mean (95% CI)

[d]ID, Iron deficiency, defined as PF < 15 µg/L

[e]Anemia, defined as Hb < 120 g/L

[f]IDA, iron deficiency anemia, defined as PF < 15 µg/L and Hb < 120 g/L

Table S4. Process design formulation parameters and loadings for MPs used in the second human study. Loading values are mean ± SD.

Human study 2 MPs				
	Fe-HA MPs (Spray dry)		**Fe-HA-BMC MPs (Spinning disc)**	
Fe isotope (mg of Fe/g of MP)	$FeSO_4$ feed (g)	HA feed (g)	HA-Fe feed (g)	BMC feed (g)
^{54}Fe (31.9 ± 0.7 mg/g)	5.57 (1.98g ^{54}Fe)	9.84	9.23	19.44
^{57}Fe (182.9 ± 3.8 mg/g)	3.78 (1.41g ^{57}Fe)	1.89	3.57	0.32
^{57}Fe (87.5 ± 1.0 mg/g)	0.80 (0.30g ^{57}Fe)	2.35	N/A	N/A
	VitA-BMC MPs (Spinning disc collected in starch bed)			
Vitamin A isotope (mg of Fe/g of MP	**VitA feed (g)**		**BMC feed (g)**	
Vitamin A (34 ± 2.4 mg/g)	54		1026	

Table S5. Quality control tests for MPs used in both human studies. Loading values are mean ± SD. CFU = Colony forming units; LAL = Limulus Amebocyte Lysate; ppm = parts per millions; USP = United States Pharmacopeia

Human study 1 MPs								
Formulation (Loading)	**Quality control tests**							
Fe isotope (mg of Fe/g of MP)	Kinetic-Chromogenic LAL Testing	Bioburden (Aerobic)	Bioburden (Soybean-Casein Digest Agar/Tryptic Soy Agar)	Bioburden (Sabouraud-Dextrose Agar)	ppm of DCM USP <467>	ppm of Residual Acetone USP <467>	ppm of Residual Ethanol USP <467>	ppm of Residual Hexane USP <467>
^{54}Fe (6.81 ± 0.13 mg/g)	< 0.047 EU/mg	< 1 CFU/ml	< 1 CFU/ml	< 1 CFU/ml	< 600	< 5000	< 5000	< 41
^{57}Fe (6.09 ± 0.20 mg/g)	< 0.004 EU/mg	< 1 CFU/ml	< 1 CFU/ml	< 1 CFU/ml	< 600	< 5000	< 5000	< 41

Human study 2 MPs				
Formulation (Loading)	**Quality control tests**			
Fe isotope (mg of Fe/g of MP)	LAL Bacterial Endotoxin (USP 40 <85>)	Bioburden (Aerobic) (USP 40 <61>)	Bioburden (Yeast-Mold) (USP 40 <61>)	ppm of DCM
^{54}Fe (31.9 ± 0.7 mg/g)	< 0.0500 EU/mg	100 CFU/g	< 100 CFU/g	131
^{57}Fe (182.9 ± 3.8 mg/g)	< 5.00 EU/mg	< 100 CFU/g	100 CFU/g	< 138